

Asymptotic theory of in-context learning by linear attention

Yue M. Lu^{*a}, Mary I. Letey^a, Jacob A. Zavatore-Veth^{†a,b,c}, Anindita Maiti^{†d}, and
Cengiz Pehlevan^{*a,c,e}

^a*The John A. Paulson School of Engineering and Applied Sciences, Harvard University*

^b*Department of Physics, Harvard University*

^c*Center for Brain Science, Harvard University*

^d*Perimeter Institute for Theoretical Physics*

^e*The Kempner Institute for the Study of Natural and Artificial Intelligence, Harvard University*

May 19, 2024

Abstract

Transformers have a remarkable ability to learn and execute tasks based on examples provided within the input itself, without explicit prior training. It has been argued that this capability, known as in-context learning (ICL), is a cornerstone of Transformers’ success, yet questions about the necessary sample complexity, pretraining task diversity, and context length for successful ICL remain unresolved. Here, we provide a precise answer to these questions in an exactly solvable model of ICL of a linear regression task by linear attention. We derive sharp asymptotics for the learning curve in a phenomenologically-rich scaling regime where the token dimension is taken to infinity; the context length and pretraining task diversity scale proportionally with the token dimension; and the number of pretraining examples scales quadratically. We demonstrate a double-descent learning curve with increasing pretraining examples, and uncover a phase transition in the model’s behavior between low and high task diversity regimes: In the low diversity regime, the model tends toward memorization of training tasks, whereas in the high diversity regime, it achieves genuine in-context learning and generalization beyond the scope of pretrained tasks. These theoretical insights are empirically validated through experiments with both linear attention and full nonlinear Transformer architectures.

1 Introduction

Since their introduction by Vaswani et al. in 2017 [1], Transformers have become a cornerstone of modern artificial intelligence (AI). Originally designed for sequence modeling tasks, such as language modeling and machine translation, Transformers achieve state-of-the-art performance across many domains, even those that are not inherently sequential [2]. Most strikingly, they underpin the breakthroughs achieved by large language models such as BERT [3], LLaMA [4], and the GPT series [5–8].

^{*}To whom correspondence should be addressed. E-mail: (Y.M.L.) yuelu@seas.harvard.edu and (C.P.) cpehlevan@seas.harvard.edu

[†]J.A.Z-V.(Author Three) contributed equally to this work with A.M. (Author Four)

The technological advancements enabled by Transformers have inspired a substantial body of research aimed at understanding their working principles. One key observation is that language models gain new behaviors and skills as their number of parameters and the size of their training datasets grow [7, 9–11]. A particularly important emergent skill is *in-context learning* (ICL), which describes the model’s ability to learn and execute tasks based on the context provided within the input itself, without the need for explicit prior training on those specific tasks. To give an example from natural language processing, a pretrained large language model might be able to successfully translate English to Italian after being prompted with a few example translations, even if it has not been specifically pretrained on that translation task [7]. ICL enables language models to perform new, specialized tasks without retraining, which is arguably a key reason for their general-purpose abilities.

Despite many recent studies on understanding ICL, important questions about how and when ICL emerges in large language models are still mostly open. Large language models are trained (or pretrained) with a next token prediction objective. How do the different algorithmic and hyperparameter choices that go into the pretraining procedure affect ICL performance? What algorithms do Transformers implement for ICL? How many pretraining examples are required for ICL to emerge? How many examples should be provided within the input for the model to be able to solve an in-context task? How diverse should the tasks in the training dataset be for in-context learning of truly new tasks not observed in the training dataset?

In this paper, we address these questions by investigating the ICL capabilities of a linear attention module for linear regression tasks. This model setting allows us to derive an asymptotically precise theory of the learning curve. In the remainder of this section, we first provide a comprehensive overview of related works on ICL. Following this, we summarize our main contributions.

1.1 Related Works

ICL in Transformer architectures. The striking ICL abilities of Transformers were thrust to the fore by Brown et al. [7]’s work on GPT-3. Focusing on natural language processing (NLP) tasks, they showed that ICL performance dramatically improves with an increase in the number of model parameters, with an increase in the number of examples in the model’s context, and with the addition of a natural language task description. In subsequent work, Wei et al. [11] proposed that the emergence of ICL with increasing scale is an abrupt, unpredictable transition. This perspective has substantially influenced proposed accounts for the emergence of ICL [12]. However, Schaeffer et al. [13] have disputed the idea that the emergence of ICL is unpredictable; they suggest that appropriately-chosen measures of otherwise hidden progress [14] reveal that ICL gradually develops with scale.

Empirical studies of synthetic ICL tasks. Though ICL in NLP is both impressive and useful, these natural data do not allow precise experimental control. Towards a fine-grained understanding of the conditions required for ICL, many recent works have explored ICL of parametrically-controllable synthetic tasks, notably linear regression and classification. These works have identified various features of pretraining data distributions that contribute to the emergence of ICL [15–19]. Closely related to our work is a study of ICL of linear regression by Raventós et al. [18]. Their work identified a task diversity threshold for the emergence of ICL, below which a pretrained Transformer behaves as a Bayesian estimator with prior determined by the limited set of pretraining tasks. Above this threshold, the model’s performance matches that of within-context ridge regression, corresponding to a Gaussian prior over all tasks, including those not seen during pretraining. This work underscores the roles of task diversity, regularization, model capacity, and data structure

in the emergence of ICL; a motivating objective of our work is to provide a theoretical account of their results.

Theoretical studies of ICL. Many theoretical studies of ICL have centered on the idea that Transformers learn a particular algorithm during pretraining, which is then flexibly deployed to solve in-context tasks. In broad strokes, papers from this program of research often consider a particular algorithm for solving an in-context task, prove that Transformers can approximately implement this algorithm, and then empirically compare the ICL performance of a pre-trained Transformer to the performance of that algorithm [20–27]. A clear consensus on which algorithm underlies ICL of linear regression in full transformers has yet to emerge [20–27]. Within this line of research, closest to our work are a series of papers that consider ICL of linear regression by simplified Transformers using linear, rather than softmax, attention modules [23, 25–30]. Zhang et al. [27] study these models in the limit of infinite pretraining dataset size (*i.e.*, the population risk limit), and show that their performance on in-context linear regression nearly matches that of the Bayes-optimal estimator for the ICL task. However, they found that linear Transformers are not robust to shifts in the within-context covariate distribution. Zhang et al. [26] then showed that any optimizer of the within-context risk for a linear Transformer solves the ICL task with an approximation to one step of gradient descent from a learnable initialization, and that the resulting estimator can saturate the Bayes error for tasks with a Gaussian prior and non-zero mean. As we will discuss in Section 2, our reduction of the linear attention module is inspired in part by these works. In very recent work, Duraisamy [30] has studied the fine-sample risk of in-context linear regression with a single step of gradient descent, without directly analyzing Transformers. Ahn et al. [23] and Wu et al. [28] investigated how linear Transformers adapt to limited pretraining data and context length, again showing that in certain cases nearly-optimal error is achievable. Like these studies, our work considers linear attention, but our analysis, with its asymptotically sharp predictions of the ICL performance, allows us to pinpoint when and how the transition from memorization to ICL of linear regression occurs. We thus in closing highlight work by Reddy [19] on in-context classification, who analyzed the transition to ICL using a phenomenological model.

1.2 Summary of contributions

We now summarize the primary contributions of our paper, relative to the prior art reviewed above. Following the recent literature, we focus on a simplified model of a Transformer that captures its key architectural motif: the linear self-attention module [23, 25–29]. Linear attention includes the quadratic interaction between inputs that lies at the heart of softmax attention, but does not include the normalization steps or fully-connected layers. This simplification makes the model more amenable for theoretical analysis. Our main result is a sharp asymptotic analysis of ICL of linear regression by linear attention, resulting in a more precisely predictive theory than previous population risk analyses or finite-sample bounds [26, 27]. The main contributions of our paper are structured as follows:

1. We begin in §2 by developing a simplified parameterization of linear self-attention that allows pretraining on the ICL linear regression task to be performed using ridge regression.
2. Within this simplified model, it is easy to identify the non-trivial scaling limit in which performance should be analyzed (§3): as the token dimension tends to infinity, the number of pretraining examples should scale quadratically (with the token dimension), while the context length and pretraining task diversity should scale linearly. In this joint limit, we can compute sharp asymptotics for ICL performance using random matrix theory.

3. Our theoretical results reveal several interesting phenomena (§3). First, we observe double-descent in the model’s ICL generalization performance as a function of pretraining dataset size, reflecting our assumption that it is pretrained to interpolation. Second, we uncover a transition to in-context learning as the pretraining task diversity increases. Concretely, there is a threshold task diversity above which linear attention saturates the Bayes error for the ICL regression task. Below that threshold, the model tends to memorize the limited set of pretraining tasks, and its excess risk is substantial. This transition recapitulates the empirical findings of Raventós et al. [18] in full Transformer models.
4. In §4, we show through numerical experiments that the insights from our theory derived on a simplified model transfer to full Transformer models with softmax self-attention. In particular, the scaling of pretraining sample complexity and task diversity with token dimension required for successful ICL is consistent.

More broadly, the study of solvable models is crucial for enhancing our grasp of how machine learning algorithms learn and generalize across various tasks. Understanding the mechanistic underpinnings of ICL of well-controlled synthetic tasks is an important prerequisite to understanding how it emerges from pretraining on natural data [19].

2 Problem formulation

We start by describing the setting of our study.

2.1 ICL of linear regression

In an ICL task, the model takes as input a sequence of tokens $\{x_1, y_1, x_2, y_2, \dots, x_\ell, y_\ell, x_{\ell+1}\}$, and outputs a prediction of $y_{\ell+1}$. We will often refer to an input sequence as a “context.” The pairs $\{x_i, y_i\}_{i=1}^{\ell+1}$ are i.i.d. samples from a *context-dependent* joint distribution $P(x, y)$. Hence, the model needs to gather information about $P(x, y)$ from the first ℓ examples and use this information to predict $y_{\ell+1}$ from $x_{\ell+1}$. We will refer to ℓ as the “context length”.

In this work, we focus on an approximately linear mapping between $x_i \in \mathbb{R}^d$ and $y_i \in \mathbb{R}$:

$$y_i = \langle x_i, w \rangle + \epsilon_i, \tag{1}$$

where ϵ_i is a Gaussian noise with mean zero and variance ρ , and $w \in \mathbb{R}^d$ is referred to as a task vector. We note that the task vector w is fixed within a context, but can change between different contexts. The model has to learn w from the ℓ pairs presented within the context, and use it to predict $y_{\ell+1}$ from $x_{\ell+1}$.

2.2 Linear self-attention

The model that we will analytically study is the linear self-attention block [31]. Linear self-attention takes as input an embedding matrix Z , whose columns hold the sequence tokens. The mapping of sequences to matrices is not unique. Here, following the convention in [27, 28, 31], we will embed the input sequence $\{x_1, y_1, x_2, y_2, \dots, x_\ell, y_\ell, x_{\ell+1}\}$ as:

$$Z = \begin{bmatrix} x_1 & x_2 & \dots & x_\ell & x_{\ell+1} \\ y_1 & y_2 & \dots & y_\ell & 0 \end{bmatrix} \in \mathbb{R}^{(d+1) \times (\ell+1)}, \tag{2}$$

where 0 in the lower-right corner is a token that prompts the missing value $y_{\ell+1}$ to be predicted.

For appropriately sized key, query, and value matrices K, Q, V , the output of a linear-attention block [31–33] is given by

$$A := Z + \frac{1}{\ell} VZ(KZ)^\top(QZ).$$

The output A is a matrix while our goal is to predict a scalar, $y_{\ell+1}$. Following the choice of positional encoding in eq. (2), we will take $A_{d+1, \ell+1}$, the element of A corresponding to the 0 prompt, as the prediction for $y_{\ell+1}$:

$$\hat{y} := A_{d+1, \ell+1}. \quad (3)$$

2.3 Pretraining data

The model is pretrained on n sample sequences, where the μ th sample is a collection of $\ell + 1$ vector-scalar pairs $\{x_i^\mu \in \mathbb{R}^d, y_i^\mu \in \mathbb{R}\}_{i=1}^{\ell+1}$ related by the approximate linear mapping in eq. (1): $y_i^\mu = \langle x_i^\mu, w^\mu \rangle + \epsilon_i^\mu$. Here, w^μ denotes the task vector associated with the μ th sample.

We make the following statistical assumptions:

1. x_i^μ are d -dimensional random vectors, sampled i.i.d. over both i and μ from a Gaussian distribution $\mathcal{N}(0, I_d/d)$.
2. For $1 \leq \mu \leq n$, the task vector w^μ associated with the μ th sample context is uniformly sampled from a finite set with k elements, denoted by $\{w_1, \dots, w_k\}$. The elements of this set are independently drawn once at the beginning of training from

$$w_i \sim_{\text{i.i.d.}} \text{Unif}(\mathcal{S}^{d-1}(\sqrt{d})), \quad (4)$$

where $\text{Unif}(\mathcal{S}^{d-1}(\sqrt{d}))$ denotes the uniform distribution on the sphere $\mathcal{S}^{d-1}(\sqrt{d})$ of radius \sqrt{d} . The variable k controls the task diversity in the pretraining data set. Importantly, k can be less than n , in which case the same task vector may be repeated multiple times.

3. The noise terms ϵ_i^μ are i.i.d. over both i and μ , and drawn from a normal distribution $\mathcal{N}(0, \rho)$.

We denote a sample from this distribution by $(Z, y_{\ell+1}) \sim \mathcal{P}_{\text{train}}$.

2.4 Parameter reduction

Before specifying a training procedure, it is insightful to examine the prediction mechanism of the linear attention module for the ICL task. This turns out to be a fruitful exercise, shedding light on critical questions: Can linear self-attention learn linear regression in-context? If so, what information do model parameters learn from data in solving this ICL problem? By closely examining these aspects, we can also formulate a simplified problem that lends itself to analytical study.

We start by rewriting the output of the linear attention module, eq. (3), in an alternative form. Following Zhang et al. [27], we define

$$V = \begin{bmatrix} V_{11} & v_{12} \\ v_{21}^\top & v_{22} \end{bmatrix}, \quad M = \begin{bmatrix} M_{11} & m_{12} \\ m_{21}^\top & m_{22} \end{bmatrix} := K^\top Q, \quad (5)$$

where $V_{11} \in \mathbb{R}^{d \times d}$, $v_{12}, v_{21} \in \mathbb{R}^{d \times 1}$, $v_{22} \in \mathbb{R}$, $M_{11} \in \mathbb{R}^{d \times d}$, $m_{12}, m_{21} \in \mathbb{R}^{d \times 1}$, and $m_{22} \in \mathbb{R}$. The expression we desire is

$$\hat{y} = \frac{1}{\ell} \left\langle x_{\ell+1}, v_{22} M_{11}^\top \sum_{i=1}^{\ell} y_i x_i + v_{22} m_{21} \sum_{i=1}^{\ell} y_i^2 + M_{11}^\top \sum_{i=1}^{\ell+1} x_i x_i^\top v_{21} + m_{21} \sum_{i=1}^{\ell} y_i x_i^\top v_{21} \right\rangle,$$

where $\langle \cdot, \cdot \rangle$ stands for the inner product.

This expression reveals several interesting points. First, not all parameters in (5) contribute to the output: We can ignore all the parameters except the last row of V and the first d columns of M . Second, the first term

$$\frac{1}{\ell} v_{22} M_{11}^\top \sum_{i=1}^{\ell} y_i x_i$$

offers a hint about how the linear attention module might be solving the task. The sum $\frac{1}{\ell} \sum_{i \leq \ell} y_i x_i$ is a noisy estimate of $\mathbb{E}[x x^\top] w$ for that context. Hence, if the parameters of the model are such that $v_{22} M_{11}^\top$ is approximately $\mathbb{E}[x x^\top]^{-1}$, this term alone makes a good prediction for the output. Third, the third term does not depend on outputs y , and thus does not directly contribute to the ICL task that relies on the relationship between x and y . Fourth, the last term only considers a one dimensional projection of x onto v_{21} . Because the task vectors w and x are isotropic in the statistical models that we consider, there are no special directions in the problem. Consequently, we expect the optimal v_{21} to be approximately zero by symmetry considerations.

Motivated by these observations, and for analytical tractability, we study the linear attention module with the constraint $v_{21} = 0$. In this case, collecting the remaining parameters in a matrix

$$\Gamma := v_{22} \begin{bmatrix} M_{11}^\top/d & m_{21} \end{bmatrix} \in \mathbb{R}^{d \times (d+1)} \quad (6)$$

and the input sequence in another matrix H_Z , defined as

$$H_Z := x_{\ell+1} \begin{bmatrix} \frac{d}{\ell} \sum_{i \leq \ell} y_i x_i^\top & \frac{1}{\ell} \sum_{i \leq \ell} y_i^2 \end{bmatrix} \in \mathbb{R}^{d \times (d+1)}, \quad (7)$$

we can rewrite the predicted label as

$$\hat{y} = \langle \Gamma, H_Z \rangle. \quad (8)$$

The $1/d$ scaling of M_{11} in Γ is chosen so that the columns of H_Z scale similarly; it does not affect the final predictor \hat{y} .

We note that Zhang et al. [27] provide an analysis of population risk (whereas we focus on empirical risk) for a related reduced model in which they set $v_{21} = 0$ and $m_{21} = 0$. Consequently, the predictors they study differ from ours (8) by an additive term. They justify this choice through an optimization argument: if these parameters are initialized to zero, they remain zero under gradient descent optimization of the population risk, given certain conditions.

In the remainder of this paper, we will examine the ICL performance of the reduced model given in (7) and (8), except when making comparisons to a full, nonlinear Transformer architecture. Henceforth, unless explicitly stated otherwise, we will refer to this reduced model as the linear attention module.

2.5 Model pretraining

The parameters of the linear attention module are learned from n samples of input sequences,

$$\{x_1^\mu, y_1^\mu, \dots, x_{\ell+1}^\mu, y_{\ell+1}^\mu\}, \quad \mu = 1, \dots, n.$$

We estimate model parameters using ridge regression, giving

$$\Gamma^* = \arg \min_{\Gamma} \sum_{\mu=1}^n \left(y_{\ell+1}^{\mu} - \langle \Gamma, H_{Z^{\mu}} \rangle \right)^2 + \frac{n}{d} \lambda \|\Gamma\|_{\text{F}}^2, \quad (9)$$

where $\lambda > 0$ is a regularization parameter, and $H_{Z^{\mu}}$ refers to the input matrix (7) populated with the μ th sample sequence. The factor n/d in front of λ makes sure that, when we take the $d \rightarrow \infty$ or $n \rightarrow \infty$ limits later, there is still a meaningful ridge regularization. The solution to the optimization problem in (9) can be expressed explicitly as

$$\text{vec}(\Gamma^*) = \left[\frac{n}{d} \lambda I + \sum_{\mu=1}^n \text{vec}(H_{Z^{\mu}}) \text{vec}(H_{Z^{\mu}})^{\top} \right]^{-1} \sum_{\mu=1}^n y_{\ell+1}^{\mu} \text{vec}(H_{Z^{\mu}}),$$

where $\text{vec}(\cdot)$ denotes the vectorization operation. Throughout this paper, we adopt the *row-major* convention. Thus, for a $d_1 \times d_2$ matrix A , $\text{vec}(A)$ is a vector in $\mathbb{R}^{d_1 d_2}$, formed by stacking the rows of A together.

2.6 Evaluation

For a given set of parameters Γ , the model’s generalization error is defined as

$$e(\Gamma) = \mathbb{E}_{\mathcal{P}_{\mathbf{s}}} \left[\left(y_{\ell+1} - \langle \Gamma, H_Z \rangle \right)^2 \right],$$

where $(Z, y_{\ell+1}) \sim \mathcal{P}_{\text{test}}$ is a new sample drawn from the distribution of the test data set. We consider two different test data distributions $\mathcal{P}_{\text{test}}$:

1. *ICL task*: x_i and ϵ_i are i.i.d. Gaussians as in the pretraining case. However, for each $1 \leq \mu \leq n$, the task vector w^{μ} associated with the μ th input sequence is drawn independently from $\text{Unif}(\mathcal{S}^{d-1}(\sqrt{d}))$. We will denote the test error under this setting by $e^{\text{ICL}}(\Gamma)$.
2. *In-distribution generalization (IDG) task*: The test data are generated in exactly the same manner as the training data, *i.e.*, $\mathcal{P}_{\text{test}} = \mathcal{P}_{\text{train}}$, hence the term in-distribution generalization. In particular, the set of unique task vectors $\{w_1, \dots, w_k\}$ is identical to that used in the pretraining data. We will denote the test error under this setting by $e^{\text{IDG}}(\Gamma)$.

The ICL task evaluates the true in-context learning performance of the linear attention module. The task vectors in the test set differ from those seen in training, requiring the model to infer them from context. The IDG task assesses the model’s performance on task vectors encountered during pretraining. High performance on the IDG task but low performance on the ICL task indicates that the model memorizes the training task vectors. Conversely, high performance on the ICL task indicates that the model can learn task vectors from the provided context.

To understand the performance of our model on both ICL and IDG tasks, we will need to evaluate these expressions for the pretrained attention matrix Γ^* . An asymptotically precise prediction of $e^{\text{ICL}}(\Gamma^*)$ and $e^{\text{IDG}}(\Gamma^*)$ will be a main result of this work.

2.7 Bayes optimal estimators

Following Raventós et al. [18], it is useful to compare the predictions made by the trained linear attention to optimal estimators that use only the current context information. These estimators do

not rely on data outside of the given context for their predictions. Under the mean square loss, the optimal Bayesian estimator $\hat{y}_{\text{Bayes}} = \mathbb{E}_{\mathcal{P}_{\mathbf{s}}} [y_{\ell+1} | x_1, y_1, x_2, y_2, \dots, x_{\ell}, y_{\ell}, x_{\ell+1}]$ in our setting has the form

$$\hat{y}_{\text{Bayes}} = (w^{\text{Bayes}})^{\top} x_{\ell+1},$$

where w^{Bayes} is the Bayes estimator of the task vector w .

For the ICL task, the Bayes-optimal ridge regression estimator is given by

$$w_{\text{ridge}}^{\text{Bayes}} := \left(\sum_{i=1}^{\ell} x_i x_i^{\top} + \rho I_d \right)^{-1} \left(\sum_{i=1}^{\ell} y_i x_i \right),$$

where the ridge is set to the noise variance ρ . We will refer to it as the *ridge estimator*. For the IDG task, the Bayes-optimal estimator is given by

$$w_{\text{dMMSE}}^{\text{Bayes}} := \frac{\sum_{j=1}^k w_j e^{-\frac{1}{2\rho} \sum_{i=1}^{\ell} (y_i - w_j^{\top} x_i)^2}}{\sum_{j=1}^k e^{-\frac{1}{2\rho} \sum_{i=1}^{\ell} (y_i - w_j^{\top} x_i)^2}}. \quad (10)$$

Here, we assume that the training task vectors $\{w_1, \dots, w_k\}$ are known to the estimator. Following [18], we will refer to this estimator as the *discrete minimum mean squared error (dMMSE) estimator*.

The test performance of these estimators are calculated by

$$e^{\text{Bayes}} = \mathbb{E}_{\mathcal{P}_{\mathbf{s}}} \left[\left(y_{\ell+1} - (w^{\text{Bayes}})^{\top} x_{\ell+1} \right)^2 \right],$$

where $\mathcal{P}_{\text{test}}$ can be the ICL or IDG task, and w^{Bayes} can be the ridge or the dMMSE estimator. To avoid possible confusion, we emphasize that we will sometimes plot the performance of an estimator on a task for which it is not optimal. For example, we will test the dMMSE estimator, which is Bayes-optimal for the pretraining distribution, on the ICL task, where it is not optimal. This will be done for benchmarking purposes.

3 Theoretical results

To answer the questions raised in the introduction, we provide a precise asymptotic analysis of the learning curves of the linear attention module for ICL of linear regression. We then verify through simulations that the primary insights gained from our theoretical analysis extend to more realistic nonlinear Transformers.

3.1 Joint asymptotic limit

We have now defined both the structure of the training data as well as the parameters to be optimized. For our theoretical analysis, we consider a joint asymptotic limit in which the input dimension d , the pretraining dataset size n , the context length ℓ , and number of task vectors in the training set k , go to infinity together such that

$$\frac{\ell}{d} := \alpha = \Theta(1), \quad \frac{k}{d} := \kappa = \Theta(1), \quad \frac{n}{d^2} := \tau = \Theta(1). \quad (11)$$

Identification of these scalings constitutes one of the main results of our paper. As we will see, the linear attention module exhibits rich learning phenomena in this limit.

The intuition for these scaling parameters can be seen as follows. Standard results in linear regression [34–36] show that to estimate a d -dimensional task vector w from the ℓ samples within a context, one needs at least $\ell = \Theta(d)$. The number of unique task vectors that must be seen to estimate the true d -dimensional Gaussian task distribution should also scale with d , *i.e.* $k = \Theta(d)$. Finally, we see from (6) that the number of linear attention parameters to be learned is $\Theta(d^2)$. This suggests that the number of individual contexts the model sees during pretraining should scale similarly, *i.e.*, $n = \Theta(d^2)$.

3.2 Learning curves for ICL of linear regression by a linear attention module

Our theoretical analysis, explained in detail in the Supplementary Information, leads to asymptotically precise expressions for the generalization error under the two test distributions under study. Specifically, our theory predicts that, as $d, n, \ell, k \rightarrow \infty$ in the joint limit given in (11),

$$e^{\text{ICL}}(\Gamma^*) \longrightarrow e^{\text{ICL}}(\tau, \alpha, \kappa, \rho, \lambda) \quad \text{almost surely,}$$

and

$$e^{\text{IDG}}(\Gamma^*) \longrightarrow e^{\text{IDG}}(\tau, \alpha, \kappa, \rho, \lambda) \quad \text{almost surely,}$$

where $e^{\text{ICL}}(\tau, \alpha, \kappa, \rho, \lambda)$ and $e^{\text{IDG}}(\tau, \alpha, \kappa, \rho, \lambda)$ are two deterministic functions of the parameters τ , α , κ , ρ and λ . The exact expressions of these two functions can be found in SI.5.2 and SI.5.3, respectively. For simplicity, we only present in what follows the ridgeless limit (*i.e.*, $\lambda \rightarrow 0^+$) of the asymptotic generalization errors.

Result 1 (ICL generalization error in the ridgeless limit). *Let*

$$q^* := \frac{1 + \rho}{\alpha}, \quad m^* := \mathcal{M}_\kappa(q^*), \quad \text{and} \quad \mu^* := q^* \mathcal{M}_{\kappa/\tau}(q^*), \quad (12)$$

where $\mathcal{M}_\kappa(\cdot)$, defined in (B.3), is a function related to the Stieltjes transform of the Marchenko-Pastur law. Then

$$\begin{aligned} e_{\text{ridgeless}}^{\text{ICL}} &:= \lim_{\lambda \rightarrow 0^+} e^{\text{ICL}}(\tau, \alpha, \kappa, \rho, \lambda) \\ &= \begin{cases} \frac{\tau(1+q^*)}{1-\tau} [1 - \tau(1 - \mu^*)^2 + \mu^*(\rho/q^* - 1)] - 2\tau(1 - \mu^*) + (1 + \rho) & \tau < 1 \\ (q^* + 1) \left(1 - 2q^*m^* - (q^*)^2 \mathcal{M}'_\kappa(q^*) + \frac{(\rho + q^* - (q^*)^2 m^*)m^*}{\tau - 1} \right) - 2(1 - q^*m^*) + (1 + \rho) & \tau > 1 \end{cases}, \end{aligned}$$

where $\mathcal{M}'_\kappa(\cdot)$ denotes the derivative of $\mathcal{M}_\kappa(q)$ with respect to q .

Result 2 (IDG generalization error in the ridgeless limit). *Let q^* , m^* , and μ^* be the scalars defined in (12). We have*

$$\begin{aligned} e_{\text{ridgeless}}^{\text{IDG}} &:= \lim_{\lambda \rightarrow 0^+} e^{\text{IDG}}(\tau, \alpha, \kappa, \rho, \lambda) \\ &= \begin{cases} \frac{\tau}{1-\tau} \left(\frac{\rho + q^* - 2q^*(1-\tau)(q^*/\xi^* + 1)}{1 - p^*(1-\tau)} + \frac{\tau\mu^*(q^* + \xi^*)^2}{q^*} \right) & \tau < 1 \\ \frac{\tau}{\tau-1} [\rho + q^*(1 - q^*m^*)] & \tau > 1 \end{cases}, \end{aligned}$$

where $\xi^* = \frac{(1-\tau)q^*}{\tau\mu^*}$ and $p^* = (1 - \kappa(\frac{\kappa\xi^*}{1-\tau} + 1)^{-2})^{-1}$.

We derive these results using techniques from random matrix theory. The full setup and technical details are presented in the Supplementary Information in [SI.1](#) through [SI.5](#). A key technical component of our analysis involves characterizing the spectral properties of the sample covariance matrix of $n = \Theta(d^2)$ i.i.d. random vectors in dimension $\Theta(d^2)$. Each of these vectors is constructed as the vectorized version of the matrix in (7). Related but simpler versions of this type of random matrices involving the tensor product of i.i.d. random vectors have been studied in recent work [37]. Some of our derivations are based on non-rigorous yet technically plausible heuristics. We support these predictions with numerical simulations and discuss in the Supplementary Information the steps required to achieve a fully rigorous proof.

Before discussing the implications of our theoretical results, we first note that if we take the limit of $\kappa \rightarrow \infty$ and $\alpha \rightarrow \infty$ in Result 1 (in either order), the ICL generalization error reduces to the generalization error of simple ridgeless interpolation with isotropic Gaussian covariates in d^2 dimensions [36, 38]:

$$\lim_{\alpha \rightarrow \infty} \lim_{\kappa \rightarrow \infty} e_{\text{ridgeless}}^{\text{ICL}} = \lim_{\kappa \rightarrow \infty} \lim_{\alpha \rightarrow \infty} e_{\text{ridgeless}}^{\text{ICL}} = \begin{cases} 1 - \tau + \frac{\rho}{1 - \tau} & \tau < 1, \\ \frac{\rho\tau}{\tau - 1} & \tau > 1. \end{cases}$$

This limiting result makes sense, given that in this limit the ICL generalization problem reduces to the generalization error of ridge regression in d^2 dimensions with covariates formed as the tensor product of i.i.d. Gaussian vectors, which by universality results in [37] should in turn be asymptotically equal to that for isotropic Gaussian covariates [36].

3.3 Sample-wise double-descent

How large should n , the pretraining dataset size, be for the linear attention to successfully learn the ICL and IDG tasks? In Figure 1, we plot our theoretical predictions for the ICL and IDG generalization error as a function of $\tau = n/d^2$ and verify them with numerical simulations. Our results demonstrate that the quadratic scaling of sample size with input dimensions is indeed the appropriate regime for nontrivial learning phenomena to occur.

As apparent in Figure 1, we find that the generalization error for both ICL and IDG tasks are not monotonic in the number of samples. In the ridgeless limit, both ICL and IDG errors diverge at $\tau = 1$, with the leading order behavior in the $\tau \uparrow 1$ (respectively $\tau \downarrow 1$) limit given by $\frac{c_1}{1-\tau}$ (respectively $\frac{c_2}{\tau-1}$), where c_1 (respectively c_2) is a τ -independent constant. This leads to a “double-descent” behavior [36, 39] in the number of samples. As in other models exhibiting double-descent [36, 38, 39], the location of the divergence is at the interpolation threshold: the number of parameters of the model (elements of Γ) is, to leading order in d , equal to d^2 , which matches the number of pretraining samples at $\tau = 1$. Further, we can investigate the effect of ridge regularisation on the steepness of the double descent, as illustrated in Figure 1c for the ICL task. As we would expect from other models exhibiting double-descent [36, 38, 39], increasing the regularization strength suppresses the peak in error around the interpolation threshold.

3.4 The ICL error can have non-monotonic dependence on context length

How large should the context length be? In Figure 2, we plot our theoretical results verified with experiments. We observe that we have correctly identified the regime where ICL appears: context length scales linearly with input dimensions. An interesting observation is that the ICL error does not always monotonically decrease with context length. There are parameter configurations with $\kappa < 1$ (blue curve in Figure 2a) for which the ICL error is minimal at some finite α .

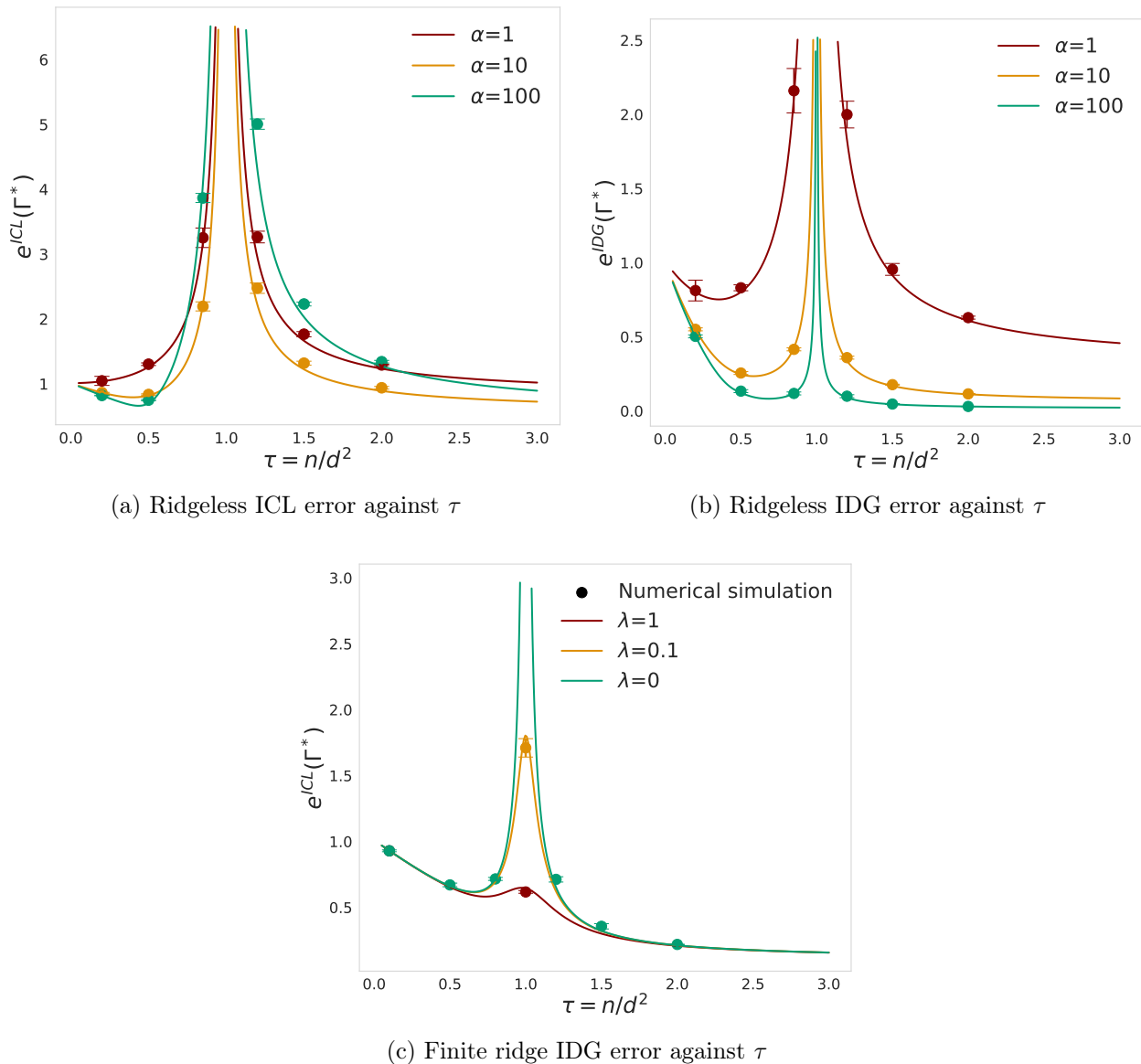


Figure 1: ICL performance as a function of τ : theory (solid lines) vs simulations (dots). Plots of (a), (c) ICL error $e^{\text{ICL}}(\Gamma^*)$ and (b) IDG error $e^{\text{IDG}}(\Gamma^*)$ vs τ at optimal Γ^* . Parameters: $d = 80, \kappa = 0.5$, and $\rho = 0.01$. Averages and standard deviations are computed over 10 runs.

3.5 Memorization to ICL transition with increasing pretraining task diversity

Recall that the parameter $\kappa = k/d$ controls the diversity of the training task vectors. How large should it be for ICL to emerge? Our theory corroborates a phenomenon that was empirically observed in a recent study [18]. Figure 3 shows a transition in the nature of the predictions that the linear attention module makes. For low κ , the model’s performance is close to that of the dMMSE estimator. This indicates that the model inherently assumes the task vector is one of the k vectors encountered in its pretraining dataset, effectively memorizing these task vectors. As κ increases beyond 1, the model’s performance approaches that of the ridge estimator. In this regime, the model generalizes to task vectors beyond its pretraining dataset, behaving as if it has learned the true prior on the task vectors despite having only seen a finite subset in the pretraining dataset.

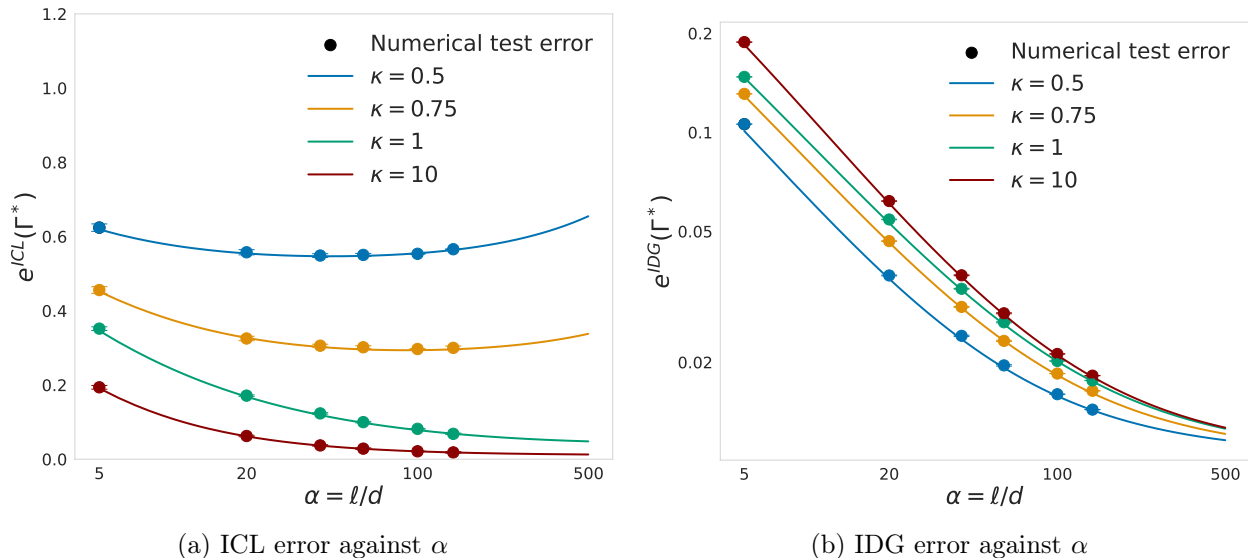


Figure 2: ICL performance as a function of α : theory (solid lines) vs simulations (dots). Plots of (a) ICL error $e_g^{\text{ICL}}(\Gamma^*)$ and (b) IDG error $e_g^{\text{IDG}}(\Gamma^*)$ vs α at optimal Γ^* . We highlight that, while the IDG error is monotonic in α , the ICL error for $\kappa = 0.5$ and $\kappa = 0.75$ is non-monotonic. *Parameters:* $d = 70, \tau = 20, \rho = 0.01$, ridgeless. Averages and standard deviations are computed over 10 runs.

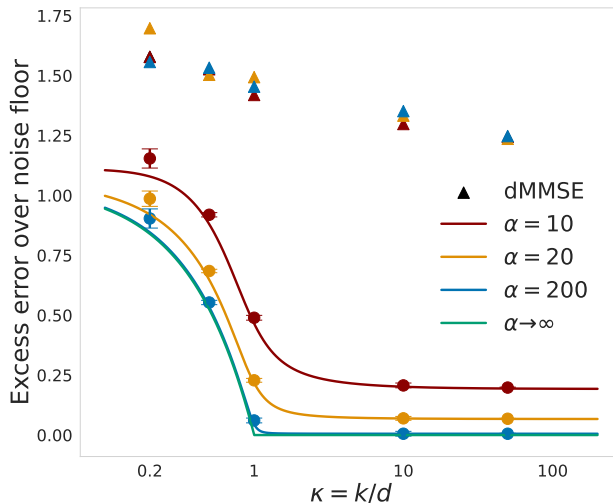
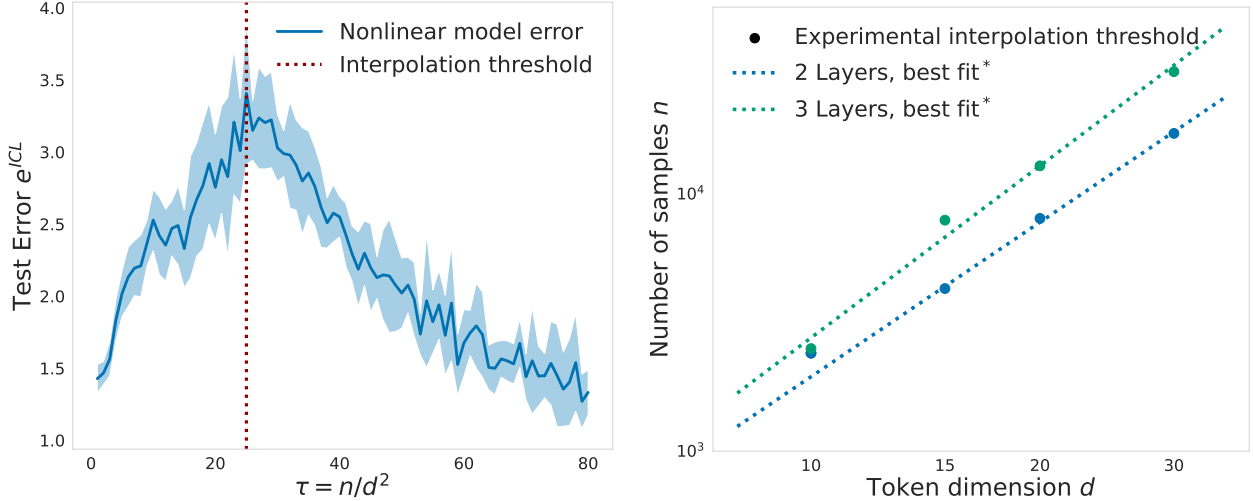


Figure 3: Comparison of linear Transformer generalization error with the dMMSE estimator given by eq. (10): theory (solid lines) vs simulations (dots, triangles). Each value plotted is the excess value of generalisation error over the noise level ρ . *Parameters:* $\tau = 0.2\alpha, \rho = 0.01$, ridgeless. Averages and standard deviations for linear model are computed over 10 runs.

To further understand the role of κ in the solution learned by the linear attention mechanism, consider the regime where $\tau, \alpha \rightarrow \infty$ with $\tau/\alpha = c^*$ kept fixed. Under this setting, we have

$$\lim_{\substack{\tau \rightarrow \infty \\ \alpha \rightarrow \infty}} e_{\text{ridgeless}}^{\text{ICL}} = \begin{cases} \rho + (1 - \kappa) \left(1 + \frac{\rho}{1 + \rho} c^*\right) & \kappa < 1 \\ \rho & \kappa > 1 \end{cases}.$$

This change in analytical behavior indicates a phase transition at $\kappa = 1$. Further, the $\kappa > 1$



(a) Nonlinear model exhibits double descent of test ICL error in scaling parameter τ . (b) Interpolation threshold follows predicted $n \propto d^2$ scaling.

Figure 4: Experimental verification of both scaling definitions and double descent behaviour in n . Figure 4a: Increasing n will increase error until an interpolation threshold is reached. Figure 4b which occurs for n proportional to d^2 , as predicted by the linear theory. Best fit lines (*) correspond to fitting $\log(n) = a \log(d) + b$ giving $a_2 = 1.82, b_2 = 3.55$ for 2-layer model and $a_3 = 2.22, b_3 = 2.81$ for 3-layer model. Interpolation threshold was computed empirically by searching for location in τ of sharp increase in value and variance of training error at a fixed number of gradient steps. *Parameters:* $d = 10, \alpha = 5, \kappa = \infty, \rho = 0.25^2$. For fig. 4a: 2-layer architecture; variance shown comes from model trained over different samples of pretraining data; lines show averages over 10 runs and shaded region shows standard deviation.

branch approaches ρ , the error of the Bayes-optimal ridge estimator in this limit. The smooth memorization-ICL transition observed in Figure 3 for the finite α, τ case stems from this phase transition.

4 Experiments with full, nonlinear Transformers

As our theoretical results are derived in a simplified setting, we aim to test if these insights are applicable to a full, nonlinear Transformer model. Specifically, we will investigate: (1) whether we have identified the correct scaling regime for non-trivial learning in an ICL task; (2) if the full Transformer exhibits a sample-wise double descent, and whether the location of the peak error scales quadratically with input dimensions as predicted by our theory; and (3) if the transition from memorization to generalization occurs, with the transition point being around $\kappa = 1$.

Our experiments¹ are done with a standard Transformer architecture consisting of blocks with: (1) a single-head softmax self-attention with $K, Q, V \in \mathbb{R}^{hd \times \ell(d+1)}$ matrices², followed by (2) a two-layer dense MLP with GELU activation and hidden layer of size $10d$ [1]. Residual connections are used between the input vector, the pre-MLP output, and the MLP output. Each sample takes the form given by eq. (2). We use either two or three Transformer blocks before returning the final

¹Code to reproduce all experiments is available at <https://github.com/Pehlevan-Group/icl-asymptotic>.

²Provided that the hidden layer dimension hd is greater than d , it does not affect the expressivity of the attention mechanism. In our experiments, we use $h = 10$.

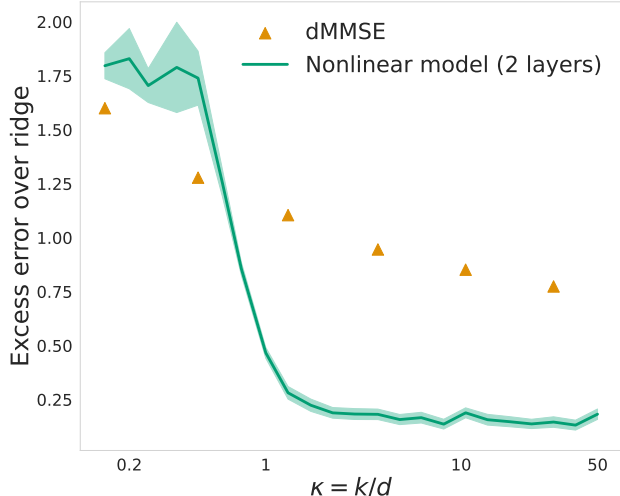


Figure 5: Experiment in 2-layer nonlinear network demonstrates a sharp transition between dMMSE estimator and ridge estimator, familiar from the linear theory. *Parameters:* $d = 20, \tau = 50, \alpha = 5, \rho = 0.01$. Variance shown comes from model trained over different samples of pretraining data; lines show averages over 10 runs and shaded region shows standard deviation.

logit corresponding to the $(d + 1, \ell + 1)$ th element in the embedding. The loss function is the mean squared error (MSE) between the predicted label (the output of the model for a given sample Z) and the true $\hat{y}_{\ell+1}$ value. We train the model in an offline setting with n samples Z_1, \dots, Z_n , using the Adam optimizer [40] with a learning rate 10^{-4} until the training error converges, typically requiring 300000-500000 gradient steps. The structure of the pretraining and test distributions exactly follows the setup described in Section 2.

In Figure 4a, we plot the generalization error and observe the double descent behavior of a full, nonlinear Transformer for the ICL task as the number of pretraining samples varies (plotted as a function of τ). We find that the peak of this curve occurs at the interpolation threshold, identified by tracking when the training loss is non-zero (see figure caption). Our theory predicts that the number of samples n at the peak of the curve, as well as the interpolation threshold, should scale with d^2 . This scaling is indeed observed in Figure 4b for the full, nonlinear Transformers. These observations suggest that the nonlinear Transformer operates within the scaling regime we have identified.

Further, as observed before in Raventós et al. [18], we recover the memorization-to-ICL transition as a function of pretraining task diversity, shown in Figure 3. We note that this transition happens near $\kappa = 1$ in the nonlinear model, consistent with our theoretical predictions on the linear model.

5 Discussion

In this paper, we computed sharp asymptotics for the in-context learning (ICL) performance in a simplified model of ICL for linear regression using linear attention. This exactly solvable model demonstrates a transition from memorizing pretraining task vectors to generalizing beyond them as the diversity of pretraining tasks increases, echoing empirical findings in full Transformers [18]. Additionally, we observe a sample-wise double descent as the amount of pretraining data increases. Our numerical experiments show that full, nonlinear Transformers exhibit similar behavior in the scaling regime relevant to our solvable model. Our work represents a first step towards a detailed

theoretical understanding of the conditions required for ICL to emerge [19].

Our paper falls within a broader program of research that seeks sharp asymptotic characterizations of the performance of machine learning algorithms. This program has a long history in statistical physics [38, 41, 42], and has in recent years attracted substantial attention in machine learning [36, 38, 43–49]. For simplicity, we have assumed that the covariates in the in-context regression problem are drawn from an isotropic Gaussian. However, our technical approach could be extended to anisotropic covariates, and, perhaps more interestingly, to featurized linear attention models in which the inputs are passed through some feature map before linear attention is applied [32, 33]. This extension would be possible thanks to an appropriate form of *Gaussian universality*: for certain classes of regression problems, the asymptotic error coincides with that of a model where the true features are replaced with Gaussian features of matched mean and covariance [36, 37, 43–48, 50]. This would allow for a theoretical characterization of ICL for realistic data structure in a close approximation of full softmax attention, yielding more precise predictions of how performance scales in real Transformers.

In our analysis, we have assumed that the model is trained to interpolation on a fixed dataset. This allows us to cast our simplified form of linear attention pretraining as a ridge regression problem, which in turn enables our random matrix analysis. In contrast, Transformer-based large language models are usually trained in a nearly-online setting, where each gradient update is estimated using fresh examples with no repeating data [51]. Some of our findings, such as double-descent in the learning curve as a function of the number of pretraining examples, are unlikely to generalize to the fully-online setting. It will be interesting to probe these potential differences in future work.

Finally, our results have some bearing on the broad question of what architectural features are required for ICL [7, 11, 19]. Our work shows that a full Transformer—or indeed even full linear attention—is not required for ICL of linear regression. However, our simplified model retains the structured quadratic interaction between inputs that is at the heart of the attention mechanism. It is this quadratic interaction that allows the model to solve the ICL regression task, which it does essentially by reversing the data correlation. One would therefore hypothesize that our model is minimal in the sense that further simplifications within this model class would impair its ability to solve this ICL task. In the specific context of regression with isotropic data, a simple point of comparison would be to fix $\Gamma = I_d$, which gives a pretraining-free model that should perform well when the context length is very long. However, this further-reduced model would perform poorly if the covariates of the in-context task are anisotropic. More generally, it would be interesting to investigate when models lacking this precisely-engineered quadratic interaction can learn linear regression in-context, and if they are less sample-efficient than the attention-based models considered here.

Acknowledgements

YML was supported by NSF Award CCF-1910410, and by the Harvard FAS Dean’s Fund for Promising Scholarship. JAZV and CP were supported by NSF Award DMS-2134157 and NSF CAREER Award IIS-2239780. CP is further supported by a Sloan Research Fellowship. AM acknowledges support from Perimeter Institute, which is supported in part by the Government of Canada through the Department of Innovation, Science and Economic Development and by the Province of Ontario through the Ministry of Colleges and Universities. This work has been made possible in part by a gift from the Chan Zuckerberg Initiative Foundation to establish the Kempner Institute for the Study of Natural and Artificial Intelligence. This research was supported in part by grants NSF PHY-1748958 and PHY-2309135 to the Kavli Institute for Theoretical Physics (KITP),

through the authors’ participation in the Fall 2023 program “Deep Learning from the Perspective of Physics and Neuroscience.”

References

- [1] Ashish Vaswani, Noam Shazeer, Niki Parmar, Jakob Uszkoreit, Llion Jones, Aidan N Gomez, Łukasz Kaiser, and Illia Polosukhin. Attention is all you need. *Advances in neural information processing systems*, 30, 2017.
- [2] Alexey Dosovitskiy, Lucas Beyer, Alexander Kolesnikov, Dirk Weissenborn, Xiaohua Zhai, Thomas Unterthiner, Mostafa Dehghani, Matthias Minderer, Georg Heigold, Sylvain Gelly, Jakob Uszkoreit, and Neil Houlsby. An image is worth 16x16 words: Transformers for image recognition at scale. *arXiv*, 2021.
- [3] Jacob Devlin, Ming-Wei Chang, Kenton Lee, and Kristina Toutanova. Bert: Pre-training of deep bidirectional transformers for language understanding. *arXiv preprint arXiv:1810.04805*, 2018.
- [4] Hugo Touvron, Thibaut Lavril, Gautier Izacard, Xavier Martinet, Marie-Anne Lachaux, Timothée Lacroix, Baptiste Rozière, Naman Goyal, Eric Hambro, Faisal Azhar, et al. Llama: Open and efficient foundation language models. *arXiv preprint arXiv:2302.13971*, 2023.
- [5] Alec Radford, Karthik Narasimhan, Tim Salimans, Ilya Sutskever, et al. Improving language understanding by generative pre-training, 2018.
- [6] Alec Radford, Jeffrey Wu, Rewon Child, David Luan, Dario Amodei, Ilya Sutskever, et al. Language models are unsupervised multitask learners. *OpenAI blog*, 1(8):9, 2019.
- [7] Tom Brown, Benjamin Mann, Nick Ryder, Melanie Subbiah, Jared D Kaplan, Prafulla Dhariwal, Arvind Neelakantan, Pranav Shyam, Girish Sastry, Amanda Askell, et al. Language models are few-shot learners. *Advances in neural information processing systems*, 33:1877–1901, 2020.
- [8] Josh Achiam, Steven Adler, Sandhini Agarwal, Lama Ahmad, Ilge Akkaya, Florencia Leoni Aleman, Diogo Almeida, Janko Altschmidt, Sam Altman, Shyamal Anadkat, et al. Gpt-4 technical report. *arXiv preprint arXiv:2303.08774*, 2023.
- [9] Deep Ganguli, Danny Hernandez, Liane Lovitt, Amanda Askell, Yuntao Bai, Anna Chen, Tom Conerly, Nova Dassarma, Dawn Drain, Nelson Elhage, et al. Predictability and surprise in large generative models. In *Proceedings of the 2022 ACM Conference on Fairness, Accountability, and Transparency*, pages 1747–1764, 2022.
- [10] Aarohi Srivastava, Abhinav Rastogi, Abhishek Rao, Abu Awal Md Shoeb, Abubakar Abid, Adam Fisch, Adam R Brown, Adam Santoro, Aditya Gupta, Adrià Garriga-Alonso, et al. Beyond the imitation game: Quantifying and extrapolating the capabilities of language models. *arXiv preprint arXiv:2206.04615*, 2022.
- [11] Jason Wei, Yi Tay, Rishi Bommasani, Colin Raffel, Barret Zoph, Sebastian Borgeaud, Dani Yogatama, Maarten Bosma, Denny Zhou, Donald Metzler, Ed H. Chi, Tatsunori Hashimoto, Oriol Vinyals, Percy Liang, Jeff Dean, and William Fedus. Emergent abilities of large language models. *Transactions on Machine Learning Research*, 2022. ISSN 2835-8856. URL <https://openreview.net/forum?id=yzkSU5zdwD>.

- [12] Catherine Olsson, Nelson Elhage, Neel Nanda, Nicholas Joseph, Nova DasSarma, Tom Henighan, Ben Mann, Amanda Askell, Yuntao Bai, Anna Chen, Tom Conerly, Dawn Drain, Deep Ganguli, Zac Hatfield-Dodds, Danny Hernandez, Scott Johnston, Andy Jones, Jackson Kernion, Liane Lovitt, Kamal Ndousse, Dario Amodei, Tom Brown, Jack Clark, Jared Kaplan, Sam McCandlish, and Chris Olah. In-context learning and induction heads. *Transformer Circuits Thread*, 2022. URL <https://transformer-circuits.pub/2022/in-context-learning-and-induction-heads/index.html>.
- [13] Rylan Schaeffer, Brando Miranda, and Sanmi Koyejo. Are emergent abilities of large language models a mirage? In *Thirty-seventh Conference on Neural Information Processing Systems*, 2023. URL <https://openreview.net/forum?id=ITw9edRD1D>.
- [14] Boaz Barak, Benjamin Edelman, Surbhi Goel, Sham Kakade, Eran Malach, and Cyril Zhang. Hidden progress in deep learning: Sgd learns parities near the computational limit. In S. Koyejo, S. Mohamed, A. Agarwal, D. Belgrave, K. Cho, and A. Oh, editors, *Advances in Neural Information Processing Systems*, volume 35, pages 21750–21764. Curran Associates, Inc., 2022. URL https://proceedings.neurips.cc/paper_files/paper/2022/file/884baf65392170763b27c914087bde01-Paper-Conference.pdf.
- [15] Stephanie C. Y. Chan, Adam Santoro, Andrew K. Lampinen, Jane X. Wang, Aaditya Singh, Pierre H. Richemond, Jay McClelland, and Felix Hill. Data distributional properties drive emergent in-context learning in transformers, 2022.
- [16] Aaditya K. Singh, Stephanie C. Y. Chan, Ted Moskovitz, Erin Grant, Andrew M. Saxe, and Felix Hill. The transient nature of emergent in-context learning in transformers, 2023.
- [17] Alberto Bietti, Vivien Cabannes, Diane Bouchacourt, Herve Jegou, and Leon Bottou. Birth of a transformer: A memory viewpoint. In A. Oh, T. Naumann, A. Globerson, K. Saenko, M. Hardt, and S. Levine, editors, *Advances in Neural Information Processing Systems*, volume 36, pages 1560–1588. Curran Associates, Inc., 2023. URL https://proceedings.neurips.cc/paper_files/paper/2023/file/0561738a239a995c8cd2ef0e50cfa4fd-Paper-Conference.pdf.
- [18] Allan Raventós, Mansheej Paul, Feng Chen, and Surya Ganguli. Pretraining task diversity and the emergence of non-bayesian in-context learning for regression. In A. Oh, T. Naumann, A. Globerson, K. Saenko, M. Hardt, and S. Levine, editors, *Advances in Neural Information Processing Systems*, volume 36, pages 14228–14246. Curran Associates, Inc., 2023. URL https://proceedings.neurips.cc/paper_files/paper/2023/file/2e10b2c2e1aa4f8083c37dfe269873f8-Paper-Conference.pdf.
- [19] Gautam Reddy. The mechanistic basis of data dependence and abrupt learning in an in-context classification task. In *The Twelfth International Conference on Learning Representations*, 2024. URL <https://openreview.net/forum?id=aN4Jf6Cx69>.
- [20] Yu Bai, Fan Chen, Huan Wang, Caiming Xiong, and Song Mei. Transformers as statisticians: Provable in-context learning with in-context algorithm selection. In A. Oh, T. Naumann, A. Globerson, K. Saenko, M. Hardt, and S. Levine, editors, *Advances in Neural Information Processing Systems*, volume 36, pages 57125–57211. Curran Associates, Inc., 2023. URL https://proceedings.neurips.cc/paper_files/paper/2023/file/b2e63e36c57e153b9015fece2352a9f9-Paper-Conference.pdf.
- [21] Yingcong Li, M. Emrullah Ildiz, Dimitris Papailiopoulos, and Samet Oymak. Transformers as algorithms: Generalization and stability in in-context learning, 2023.

- [22] Ekin Akyürek, Dale Schuurmans, Jacob Andreas, Tengyu Ma, and Denny Zhou. What learning algorithm is in-context learning? investigations with linear models. In *The Eleventh International Conference on Learning Representations*, 2023. URL <https://openreview.net/forum?id=0gOX4H8yN4I>.
- [23] Kwangjun Ahn, Xiang Cheng, Hadi Daneshmand, and Suvrit Sra. Transformers learn to implement preconditioned gradient descent for in-context learning, 2023.
- [24] Deqing Fu, Tian-Qi Chen, Robin Jia, and Vatsal Sharan. Transformers learn higher-order optimization methods for in-context learning: A study with linear models, 2023.
- [25] Johannes Von Oswald, Eyvind Niklasson, Ettore Randazzo, João Sacramento, Alexander Mordvintsev, Andrey Zhmoginov, and Max Vladymyrov. Transformers learn in-context by gradient descent. In Andreas Krause, Emma Brunskill, Kyunghyun Cho, Barbara Engelhardt, Sivan Sabato, and Jonathan Scarlett, editors, *Proceedings of the 40th International Conference on Machine Learning*, volume 202 of *Proceedings of Machine Learning Research*, pages 35151–35174. PMLR, 23–29 Jul 2023. URL <https://proceedings.mlr.press/v202/von-oswald23a.html>.
- [26] Ruiqi Zhang, Jingfeng Wu, and Peter L. Bartlett. In-context learning of a linear transformer block: Benefits of the mlp component and one-step gd initialization, 2024.
- [27] Ruiqi Zhang, Spencer Frei, and Peter L. Bartlett. Trained transformers learn linear models in-context. *Journal of Machine Learning Research*, 25(49):1–55, 2024. URL <http://jmlr.org/papers/v25/23-1042.html>.
- [28] Jingfeng Wu, Difan Zou, Zixiang Chen, Vladimir Braverman, Quanquan Gu, and Peter Bartlett. How many pretraining tasks are needed for in-context learning of linear regression? In *The Twelfth International Conference on Learning Representations*, 2024. URL <https://openreview.net/forum?id=vSh5ePa0ph>.
- [29] Pritam Chandra, Tanmay Kumar Sinha, Kabir Ahuja, Ankit Garg, and Navin Goyal. Towards analyzing self-attention via linear neural network, 2024. URL <https://openreview.net/forum?id=4fVuBf5HE9>.
- [30] Karthik Duraisamy. Finite sample analysis and bounds of generalization error of gradient descent in in-context linear regression. *arXiv preprint arXiv:2405.02462*, 2024.
- [31] Sinong Wang, Belinda Z. Li, Madian Khabsa, Han Fang, and Hao Ma. Linformer: Self-attention with linear complexity, 2020.
- [32] Zhuoran Shen, Mingyuan Zhang, Haiyu Zhao, Shuai Yi, and Hongsheng Li. Efficient attention: Attention with linear complexities. In *Proceedings of the IEEE/CVF winter conference on applications of computer vision*, pages 3531–3539, 2021.
- [33] Angelos Katharopoulos, Apoorv Vyas, Nikolaos Pappas, and François Fleuret. Transformers are RNNs: Fast autoregressive transformers with linear attention. In *International conference on machine learning*, pages 5156–5165. PMLR, 2020.
- [34] Vladimir Alexandrovich Marchenko and Leonid Andreevich Pastur. Distribution of eigenvalues for some sets of random matrices. *Matematicheskii Sbornik*, 114(4):507–536, 1967.

- [35] Zhidong Bai and Jack W Silverstein. *Spectral analysis of large dimensional random matrices*, volume 20. Springer, 2010.
- [36] Trevor Hastie, Andrea Montanari, Saharon Rosset, and Ryan J. Tibshirani. Surprises in high-dimensional ridgeless least squares interpolation. *The Annals of Statistics*, 50(2):949 – 986, 2022. doi: 10.1214/21-AOS2133. URL <https://doi.org/10.1214/21-AOS2133>.
- [37] Sofiia Dubova, Yue M. Lu, Benjamin McKenna, and Horng-Tzer Yau. Universality for the global spectrum of random inner-product kernel matrices in the polynomial regime. *arXiv*, 2023.
- [38] Alexander B. Atanasov, Jacob A. Zavatone-Veth, and Cengiz Pehlevan. Scaling and renormalization in high-dimensional regression. *arXiv*, 2024.
- [39] Mikhail Belkin, Daniel Hsu, Siyuan Ma, and Soumik Mandal. Reconciling modern machine-learning practice and the classical bias–variance trade-off. *Proceedings of the National Academy of Sciences*, 116(32):15849–15854, 2019.
- [40] Diederik Kingma and Jimmy Ba. Adam: A method for stochastic optimization. In *International Conference on Learning Representations (ICLR)*, San Diego, CA, USA, 2015.
- [41] Timothy L. H. Watkin, Albrecht Rau, and Michael Biehl. The statistical mechanics of learning a rule. *Rev. Mod. Phys.*, 65:499–556, Apr 1993. doi: 10.1103/RevModPhys.65.499. URL <https://link.aps.org/doi/10.1103/RevModPhys.65.499>.
- [42] Andreas Engel and Christian van den Broeck. *Statistical Mechanics of Learning*. Cambridge University Press, 2001. doi: <https://doi.org/10.1017/CBO9781139164542>.
- [43] Federica Gerace, Bruno Loureiro, Florent Krzakala, Marc Mézard, and Lenka Zdeborová. Generalisation error in learning with random features and the hidden manifold model. In *International Conference on Machine Learning*, pages 3452–3462. PMLR, 2020.
- [44] Bruno Loureiro, Cedric Gerbelot, Hugo Cui, Sebastian Goldt, Florent Krzakala, Marc Mezard, and Lenka Zdeborová. Learning curves of generic features maps for realistic datasets with a teacher-student model. *Advances in Neural Information Processing Systems*, 34:18137–18151, 2021.
- [45] Song Mei and Andrea Montanari. The generalization error of random features regression: Precise asymptotics and the double descent curve. *Communications on Pure and Applied Mathematics*, 75(4):667–766, 2022.
- [46] Hong Hu and Yue M Lu. Universality laws for high-dimensional learning with random features. *IEEE Transactions on Information Theory*, 69(3):1932–1964, 2022.
- [47] Hong Hu, Yue M. Lu, and Theodor Misiakiewicz. Asymptotics of random feature regression beyond the linear scaling regime. *arXiv:2403.08160*, 2024.
- [48] Oussama Dhifallah and Yue M Lu. A precise performance analysis of learning with random features. *arXiv preprint arXiv:2008.11904*, 2020.
- [49] Hugo Cui, Freya Behrens, Florent Krzakala, and Lenka Zdeborová. A phase transition between positional and semantic learning in a solvable model of dot-product attention. *arXiv*, 2024.

- [50] Andrea Montanari and Basil N. Saeed. Universality of empirical risk minimization. In Po-Ling Loh and Maxim Raginsky, editors, *Proceedings of Thirty Fifth Conference on Learning Theory*, volume 178 of *Proceedings of Machine Learning Research*, pages 4310–4312. PMLR, 02–05 Jul 2022. URL <https://proceedings.mlr.press/v178/montanari22a.html>.
- [51] Niklas Muennighoff, Alexander M Rush, Boaz Barak, Teven Le Scao, Nouamane Tazi, Aleksandra Piktus, Sampo Pyysalo, Thomas Wolf, and Colin Raffel. Scaling data-constrained language models. In *Thirty-seventh Conference on Neural Information Processing Systems*, 2023. URL <https://openreview.net/forum?id=j5BuTrEj35>.
- [52] László Erdős, Antti Knowles, Horng-Tzer Yau, and Jun Yin. The local semicircle law for a general class of random matrices. *Electronic Journal of Probability*, 18(none):1 – 58, 2013. doi: 10.1214/EJP.v18-2473. URL <https://doi.org/10.1214/EJP.v18-2473>.
- [53] László Erdős and Horng-Tzer Yau. *A dynamical approach to random matrix theory*, volume 28. American Mathematical Soc., 2017.
- [54] Alston S. Householder. Unitary triangularization of a nonsymmetric matrix. *J. ACM*, 5(4): 339–342, oct 1958. ISSN 0004-5411. doi: 10.1145/320941.320947. URL <https://doi.org/10.1145/320941.320947>.
- [55] Yue M. Lu. Householder dice: A matrix-free algorithm for simulating dynamics on Gaussian and random orthogonal ensembles. *IEEE Transactions on Information Theory*, 67(12):8264–8272, 2021. doi: 10.1109/TIT.2021.3114351.
- [56] Lloyd N. Trefethen and David Bau, III. *Numerical Linear Algebra*. Society for Industrial and Applied Mathematics, Philadelphia, PA, 1997. doi: 10.1137/1.9780898719574. URL <https://epubs.siam.org/doi/abs/10.1137/1.9780898719574>.

Supplementary Information

Some of the derivations in this document are based on non-rigorous yet technically sound heuristic arguments from random matrix theory. We support these predictions with numerical simulations and discuss the steps required to achieve a fully rigorous proof. All rigorously proven results will be clearly stated as lemmas, propositions, and the like.

SI.1 Notation

Sets, vectors and matrices: For each $n \in \mathbb{N}$, $[n] := \{1, 2, \dots, n\}$. The sphere in \mathbb{R}^d with radius \sqrt{d} is expressed as $\mathcal{S}^{d-1}(\sqrt{d})$. For a vector $v \in \mathbb{R}^d$, its ℓ_2 norm is denoted by $\|v\|$. For a matrix $A \in \mathbb{R}^{d \times d}$, $\|A\|_{\text{op}}$ and $\|A\|_{\text{F}}$ denote the operator (spectral) norm and the Frobenius norm of A , respectively. Additionally, $\|A\|_{\infty} := \max_{i,j \in [n]} |A(i, j)|$ denotes the entry-wise ℓ_{∞} norm. We use e_1 to denote the first natural basis vector $(1, 0, \dots, 0)$, and I is an identity matrix. Their dimensions can be inferred from the context. The trace of A is written as $\text{tr}(A)$.

Our derivations will frequently use the vectorization operation, denoted by $\text{vec}(\cdot)$. It maps a $d_1 \times d_2$ matrix $A \in \mathbb{R}^{d_1 \times d_2}$ to a vector $v_A = \text{vec}(A)$ in $\mathbb{R}^{d_1 d_2}$. Note that we shall adopt the *row-major* convention, and thus the rows of A are stacked together to form v_A . We also recall the standard identity:

$$\text{vec}(E_1 E_2 E_3) = (E_1 \otimes E_3^{\top}) \text{vec}(E_2), \quad (\text{SI.1.1})$$

where \otimes denotes the matrix Kronecker product, and E_1, E_2, E_3 are matrices whose dimensions are compatible for the multiplication operation. For any square matrix $A \in \mathbb{R}^{(L+1) \times (L+1)}$, we introduce the notation

$$[M]_{\setminus 0} \in \mathbb{R}^{L \times L} \quad (\text{SI.1.2})$$

to denote the principal minor of M after removing its first row and column.

Stochastic order notation: In our analysis, we use a concept of high-probability bounds known as *stochastic domination*. This notion, first introduced in [52, 53], provides a convenient way to account for low-probability exceptional events where some bounds may not hold. Consider two families of nonnegative random variables:

$$X = (X^{(d)}(u) : d \in \mathbb{N}, u \in U^{(d)}), \quad Y = (Y^{(d)}(u) : d \in \mathbb{N}, u \in U^{(d)}),$$

where $U^{(d)}$ is a possibly d -dependent parameter set. We say that X is *stochastically dominated* by Y , uniformly in u , if for every (small) $\varepsilon > 0$ and (large) $D > 0$ we have

$$\sup_{u \in U^{(d)}} \mathbb{P}[X^{(d)}(u) > d^{\varepsilon} Y^{(d)}(u)] \leq d^{-D}$$

for sufficiently large $d \geq d_0(\varepsilon, D)$. If X is stochastically dominated by Y , uniformly in u , we use the notation $X \prec Y$. Moreover, if for some family X we have $|X| \prec Y$, we also write $X = \mathcal{O}_{\prec}(Y)$.

We also use the notation $X \simeq Y$ to indicate that two families of random variables X, Y are asymptotically equivalent. Precisely, $X \simeq Y$, if there exists $\varepsilon > 0$ such that for every $D > 0$ we have

$$\mathbb{P}[|X - Y| > d^{-\varepsilon}] \leq d^{-D} \quad (\text{SI.1.3})$$

for all sufficiently large $d > d_0(\varepsilon, D)$.

SI.2 Moment Calculations and Generalization Errors

For a given set of parameters Γ , its generalization error is defined as

$$e(\Gamma) = \mathbb{E}_{\mathcal{P}_{\mathfrak{s}}} \left[(y_{\ell+1} - \langle \Gamma, H_Z \rangle)^2 \right], \quad (\text{SI.2.1})$$

where $(Z, y_{\ell+1}) \sim \mathcal{P}_{\text{test}}$ is a new sample drawn from the distribution of the test data set. Recall that Z is the input embedding matrix defined in (2) in the main text, and $y_{\ell+1}$ denotes the missing value to be predicted. The goal of this section is to derive an expression for the generalization error $e(\Gamma)$.

Note that the test distribution $\mathcal{P}_{\text{test}}$ crucially depends on the probability distribution of the task vector w used in the linear model in (1). For the ICL task, we have $w \sim \text{Unif}(\mathcal{S}^{d-1}(\sqrt{d}))$, the uniform distribution on the sphere $\mathcal{S}^{d-1}(\sqrt{d})$. For the IDG task, w is sampled uniformly from the set $\{w_1, w_2, \dots, w_k\}$, where these k vectors are the same as those used in the training data [see (4)]. In what follows, we slightly abuse the notation by writing $w \sim \mathcal{P}_{\text{test}}$ to indicate that w is sampled from the task vector distribution associated with $\mathcal{P}_{\text{test}}$.

Let w be the task vector used in the input matrix Z . Throughout the paper, we use $\mathbb{E}_w[\cdot]$ to denote the conditional expectation with respect to the randomness in the data vectors $\{x_i\}_{i \in [\ell+1]}$ and the noise $\{\epsilon_i\}_{i \in [\ell+1]}$, with the task vector w kept fixed. We have the following expressions for the first two *conditional* moments of $(H_Z, y_{\ell+1})$.

Lemma 1 (Conditional moments). *Let the task vector $w \in \mathcal{S}^{d-1}(\sqrt{d})$ be fixed. We have*

$$\mathbb{E}_w [y_{\ell+1}] = 0, \quad \text{and} \quad \mathbb{E}_w [H_Z] = 0. \quad (\text{SI.2.2})$$

Moreover,

$$\mathbb{E}_w [y_{\ell+1} H_Z] = \frac{1}{d} w \left[w^\top, \quad 1 + \rho \right] \quad (\text{SI.2.3})$$

and

$$\mathbb{E}_w \left[\text{vec}(H_Z) \text{vec}(H_Z)^\top \right] = \frac{(1 + \rho)}{d} I_d \otimes \begin{bmatrix} \frac{d}{\ell} I_d + (1 + \ell^{-1})(1 + \rho)^{-1} w w^\top & (1 + 2\ell^{-1})w \\ (1 + 2\ell^{-1})w^\top & (1 + 2\ell^{-1})(1 + \rho) \end{bmatrix}. \quad (\text{SI.2.4})$$

Proof. Using the equivalent representations in (A.1) and (A.2), it is straightforward to verify the estimates of the first (conditional) moments in (SI.2.2). To show (SI.2.3), we note that

$$H_Z = (d/\ell) z_a z_b^\top,$$

where

$$z_a = M_w \begin{bmatrix} s \\ u \end{bmatrix} \quad \text{and} \quad z_b = \begin{bmatrix} M_w h \\ (\theta_w a / \sqrt{d} + \theta_\epsilon)^2 / \sqrt{d} + \theta_q^2 / \sqrt{d} \end{bmatrix}.$$

Using the representation in (A.2), we have

$$\mathbb{E}_w [y_{\ell+1} H_Z] = (d/\ell) \mathbb{E}_w [y_{\ell+1} z_a] \mathbb{E}_w [z_b^\top].$$

Computing the expectations $\mathbb{E}_w [y_{\ell+1} z_a]$ and $\mathbb{E}_w [z_b^\top]$ then gives us (SI.2.3). Next, we show (SI.2.4). Since z_a and z_b are *independent*,

$$\mathbb{E} \left[\text{vec}(H_Z) \text{vec}(H_Z)^\top \right] = (d/\ell)^2 \mathbb{E} \left[z_a z_a^\top \right] \otimes \mathbb{E} \left[z_b z_b^\top \right].$$

The first expectation on the right-hand side is easy to compute. Since M_w is an orthonormal matrix,

$$\mathbb{E}_w \left[z_a z_a^\top \right] = I_d \quad (\text{SI.2.5})$$

To obtain the second expectation on the right-hand side of the above expression, we can first verify that

$$\mathbb{E}_w \left[M_w h h^\top M_w \right] = \frac{\ell}{d^2} \left[(1 + \rho) I_d + \frac{(\ell + 1)}{d} w w^\top \right]. \quad (\text{SI.2.6})$$

Moreover,

$$\mathbb{E}_w \left[M_w h \left((a/\sqrt{d} + \theta_\epsilon)^2 / \sqrt{d} + \theta_q^2 / \sqrt{d} \right) \right] = \frac{\ell(\ell + 2)(1 + \rho)}{d^3} w \quad (\text{SI.2.7})$$

and

$$\mathbb{E}_w \left[\left((a/\sqrt{d} + \theta_\epsilon)^2 / \sqrt{d} + \theta_q^2 / \sqrt{d} \right)^2 \right] = \frac{\ell(\ell + 2)(1 + \rho)^2}{d^3}. \quad (\text{SI.2.8})$$

Combining (SI.2.6), (SI.2.7), and (SI.2.8), we have

$$\mathbb{E} \left[z_b z_b^\top \right] = \frac{(\ell/d)^2(1 + \rho)}{d} \begin{bmatrix} \frac{d}{\ell} I_d + (1 + \ell^{-1})(1 + \rho)^{-1} w w^\top & (1 + 2\ell^{-1}) w \\ (1 + 2\ell^{-1}) w^\top & (1 + 2\ell^{-1})(1 + \rho) \end{bmatrix}. \quad (\text{SI.2.9})$$

Substituting (SI.2.5) and (SI.2.9) into (SI.2.4), we reach the formula in (SI.2.4). \square

Proposition 1 (Generalization error). *For a given weight matrix Γ , the generalization error of the linear transformer is*

$$\begin{aligned} e(\Gamma) &= \frac{1 + \rho}{d} \text{tr} \left(\Gamma \begin{bmatrix} \frac{d}{\ell} I_d + (1 + \ell^{-1})(1 + \rho)^{-1} R_{\text{test}} & (1 + 2\ell^{-1}) b_{\text{test}} \\ (1 + 2\ell^{-1}) b_{\text{test}}^\top & (1 + 2\ell^{-1})(1 + \rho) \end{bmatrix} \Gamma^\top \right) \\ &\quad - \frac{2}{d} \text{tr} \left(\Gamma \begin{bmatrix} R_{\text{test}} \\ (1 + \rho) b_{\text{test}}^\top \end{bmatrix} \right) + 1 + \rho, \end{aligned}$$

where

$$b_{\text{test}} := \mathbb{E}_{w \sim \mathcal{P}_{\mathbf{b}}} [w] \quad \text{and} \quad R_{\text{test}} := \mathbb{E}_{w \sim \mathcal{P}_{\mathbf{b}}} [w w^\top]. \quad (\text{SI.2.10})$$

Remark 1. *We use $w \sim \mathcal{P}_{\text{test}}$ to indicate that w is sampled from the task vector distribution associated with $\mathcal{P}_{\text{test}}$. Recall our discussions in Section 2.6. For the ICL task, $w \sim \text{Unif}(\mathcal{S}^{d-1}(\sqrt{d}))$. It is straightforward to check that, in this case,*

$$(\text{ICL}) : \quad b_{\text{test}} = 0 \quad \text{and} \quad R_{\text{test}} = I_d. \quad (\text{SI.2.11})$$

For the IDG task, we have

$$(\text{IDG}) : \quad b_{\text{test}} = \frac{1}{k} \sum_i w_i \quad \text{and} \quad R_{\text{test}} = \frac{1}{k} \sum_{i \in [k]} w_i w_i^\top, \quad (\text{SI.2.12})$$

where $\{w_i\}_{i \in [k]}$ is the set of fixed task vectors used in the training data.

Proof. Recall the definition of the generalization error in (SI.2.1). We start by writing

$$e(\Gamma) = \text{vec}(\Gamma)^\top \mathbb{E} \left[\text{vec}(H_Z) \text{vec}(H_Z)^\top \right] \text{vec}(\Gamma) - 2 \text{vec}(\Gamma)^\top \text{vec}(\mathbb{E} [y_{N+1} H_Z]) + \mathbb{E} \left[y_{\ell+1}^2 \right],$$

where H_Z is a matrix in the form of (7) and H_Z is independent of Γ . Since $y_{\ell+1} = x_{\ell+1}^\top w + \epsilon$, with $\epsilon \sim \mathcal{N}(0, \rho)$ denoting the noise, it is straightforward to check that

$$\mathbb{E} \left[y_{\ell+1}^2 \right] = 1 + \rho.$$

Using the moment estimate (SI.2.4) in Lemma 1 and the identity (SI.1.1), we have

$$\begin{aligned} & \text{vec}(\Gamma)^\top \mathbb{E} \left[\text{vec}(H_Z) \text{vec}(H_Z)^\top \right] \text{vec}(\Gamma) \\ &= \frac{1 + \rho}{d} \text{tr} \left(\Gamma \begin{bmatrix} \frac{d}{\ell} I_d + (1 + \ell^{-1})(1 + \rho)^{-1} R_{\text{test}} & (1 + 2\ell^{-1}) b_{\text{test}} \\ (1 + 2\ell^{-1}) b_{\text{test}}^\top & (1 + 2\ell^{-1})(1 + \rho) \end{bmatrix} \Gamma^\top \right). \end{aligned}$$

Moreover, by (SI.2.3),

$$\text{vec}(\Gamma)^\top \text{vec}(\mathbb{E} [y_{\ell+1} H_Z]) = \frac{1}{d} \text{tr} \left(\Gamma \begin{bmatrix} R_{\text{test}} \\ (1 + \rho) b_{\text{test}}^\top \end{bmatrix} \right).$$

□

Corollary 1. For a given set of parameters Γ , its generalization error can be written as

$$e(\Gamma) = \frac{1}{d} \text{tr}(\Gamma B_{\text{test}} \Gamma^\top) - \frac{2}{d} \text{tr}(\Gamma A_{\text{test}}^\top) + (1 + \rho) + \mathcal{E}, \quad (\text{SI.2.13})$$

where

$$A_{\text{test}} := \begin{bmatrix} R_{\text{test}} & (1 + \rho) b_{\text{test}} \end{bmatrix}, \quad (\text{SI.2.14})$$

$$B_{\text{test}} := \begin{bmatrix} \frac{1}{\alpha}(1 + \rho) I_d + R_{\text{test}} & (1 + \rho) b_{\text{test}} \\ (1 + \rho) b_{\text{test}}^\top & (1 + \rho)^2 \end{bmatrix}, \quad (\text{SI.2.15})$$

and $R_{\text{test}}, b_{\text{test}}$ are as defined in (SI.2.10). Moreover, \mathcal{E} denotes an “error” term such that

$$|\mathcal{E}| \leq \frac{C_{\alpha, \rho} \max \left\{ \|R_{\text{test}}\|_{\text{op}}, \|b_{\text{test}}\|, 1 \right\} \left(\|\Gamma\|_{\text{F}}^2 / d \right)}{d}, \quad (\text{SI.2.16})$$

where $C_{\alpha, \rho}$ is some constant that only depends on α and ρ .

Proof. Let

$$\Delta = \begin{bmatrix} \frac{d}{\ell}(1 + \rho) I_d + (1 + \ell^{-1}) R_{\text{test}} & (1 + 2\ell^{-1})(1 + \rho) b_{\text{test}} \\ (1 + 2\ell^{-1})(1 + \rho) b_{\text{test}}^\top & (1 + 2\ell^{-1})(1 + \rho)^2 \end{bmatrix} - B_{\text{test}}.$$

It is straightforward to check that

$$\begin{aligned} \mathcal{E} &= \frac{1}{d} \text{tr}(\Gamma \Delta \Gamma^\top) \\ &= \frac{1}{d} \text{vec}(\Gamma)^\top (I_d \otimes \Delta) \text{vec}(\Gamma) \\ &\leq \|\Delta\|_{\text{op}} \frac{\|\Gamma\|_{\text{F}}^2}{d}. \end{aligned}$$

The bound in (SI.2.16) follows from the estimate that $\|\Delta\|_{\text{op}} \leq C_{\alpha, \rho} \max \left\{ \|R_{\text{test}}\|_{\text{op}}, \|b_{\text{test}}\|, 1 \right\} / d$. □

Remark 2. Consider the optimal weight matrix Γ^* obtained by solving the ridge regression problem in (9). Since Γ^* is the optimal solution of (9), we must have

$$\frac{n}{d}\lambda\|\Gamma^*\|_{\text{F}}^2 \leq \sum_{\mu \in [n]} (y_{\ell+1}^\mu)^2,$$

where the right-hand side is the value of the objective function of (9) when we choose Γ to be the all-zero matrix. It follows that

$$\frac{\|\Gamma^*\|_{\text{F}}^2}{d} \leq \frac{\sum_{\mu \in [n]} (y_{\ell+1}^\mu)^2}{\lambda n}.$$

By the law of large numbers, $\frac{\sum_{\mu \in [n]} y_\mu^2}{n} \rightarrow 1 + \rho$ as $n \rightarrow \infty$. Thus, $\|\Gamma^*\|_{\text{F}}^2/d$ is asymptotically bounded by the constant $(1 + \rho)/\lambda$. Furthermore, it is easy to check that $\|R_{\text{test}}\|_{\text{op}} = \mathcal{O}(1)$ and $\|b_{\text{test}}\| = \mathcal{O}(1)$ for both ICL [see (SI.2.11)] and IDG [see (SI.2.12)]. It then follows from Corollary 1 that the generalization error associated with the optimal parameters Γ^* is asymptotically determined by the first three terms on the right-hand side of (SI.2.13).

SI.3 Analysis of Ridge Regression: Extended Resolvent Matrices

We see from Corollary 1 and Remark 2 that the two key quantities in determining the generalization error $e(\Gamma^*)$ are

$$\frac{1}{d} \text{tr}(\Gamma^* A_{\text{test}}^\top) \quad \text{and} \quad \frac{1}{d} \text{tr}(\Gamma^* B_{\text{test}}(\Gamma^*)^\top), \quad (\text{SI.3.1})$$

where A_{test} and B_{test} are the matrices defined in (SI.2.14) and (SI.2.15), respectively. In this section, we show that the two quantities in (SI.3.1) can be obtained by studying a parameterized family of extended resolvent matrices.

To start, we observe that the ridge regression problem in (9) admits the following closed-form solution:

$$\text{vec}(\Gamma^*) = G \left(\sum_{\mu \in [n]} y_\mu \text{vec}(H_\mu) \right) / d, \quad (\text{SI.3.2})$$

where G is a resolvent matrix defined as

$$G = \left(\sum_{\mu \in [n]} \text{vec}(H_\mu) \text{vec}(H_\mu)^\top / d + \tau \lambda I \right)^{-1}. \quad (\text{SI.3.3})$$

For our later analysis of the generalization error, we need to consider a more general, ‘‘parameterized’’ version of G , defined as

$$G(\pi) = \left(\sum_{\mu \in [n]} \text{vec}(H_\mu) \text{vec}(H_\mu)^\top / d + \pi \Omega + \tau \lambda I \right)^{-1}, \quad (\text{SI.3.4})$$

where $\Omega \in \mathbb{R}^{(d^2+d) \times (d^2+d)}$ is a symmetric positive-semidefinite matrix and π is a nonnegative scalar. The original resolvent G in (SI.3.3) is a special case, corresponding to $\pi = 0$.

The objects in (SI.3.2) and (SI.3.4) are the submatrices of an *extended* resolvent matrix, which we construct as follows. For each $\mu \in [n]$, let

$$z_\mu = \begin{bmatrix} y_\mu/d \\ \text{vec}(H_\mu)/\sqrt{d} \end{bmatrix} \quad (\text{SI.3.5})$$

be an $(d^2 + d + 1)$ -dimensional vector. Let

$$\Omega_e = \begin{bmatrix} 0 & \\ & \Omega \end{bmatrix}, \quad (\text{SI.3.6})$$

where Ω is the $(d^2 + d) \times (d^2 + d)$ matrix in (SI.3.4). Define an extended resolvent matrix

$$G_e(\pi) = \frac{1}{\sum_{\mu \in [n]} z_\mu z_\mu^\top + \pi \Omega_e + \tau \lambda I}. \quad (\text{SI.3.7})$$

By block-matrix inversion, it is straightforward to check that

$$G_e(\pi) = \begin{bmatrix} c(\pi) & -c(\pi)q^\top(\pi) \\ -c(\pi)q(\pi) & G(\pi) + c(\pi)q(\pi)q^\top(\pi) \end{bmatrix}, \quad (\text{SI.3.8})$$

where

$$q(\pi) := \frac{1}{d^{3/2}} G(\pi) \left(\sum_{\mu \in [n]} y_\mu \text{vec}(H_\mu) \right) \quad (\text{SI.3.9})$$

is a vector in $\mathbb{R}^{d(d+1)}$, and $c(\pi)$ is a scalar such that

$$\frac{1}{c(\pi)} = \frac{1}{d^2} \sum_{\mu \in [n]} y_\mu^2 + \tau \lambda - \frac{1}{d^3} \sum_{\mu, \nu \in [n]} y_\mu y_\nu \text{vec}(H_\mu)^\top G(\pi) \text{vec}(H_\nu). \quad (\text{SI.3.10})$$

By comparing (SI.3.9) with (SI.3.2), we see that

$$\text{vec}(\Gamma^*) = \sqrt{d} q(0). \quad (\text{SI.3.11})$$

Moreover, as shown in the following lemma, the two key quantities in (SI.3.1) can also be obtained from the extended resolvent $G_e(\pi)$.

Lemma 2. For any matrix $A \in \mathbb{R}^{d \times (d+1)}$,

$$\frac{1}{d} \text{tr}(\Gamma^* A^\top) = \frac{-1}{c(0)\sqrt{d}} \left[0 \quad \text{vec}(A)^\top \right] G_e(0) e_1, \quad (\text{SI.3.12})$$

where e_1 denotes the first natural basis vector in \mathbb{R}^{d^2+d+1} . Moreover, for any symmetric and positive semidefinite matrix $B \in \mathbb{R}^{(d+1) \times (d+1)}$, if we set

$$\Omega = I_d \otimes B \quad (\text{SI.3.13})$$

in (SI.3.6), then

$$\frac{1}{d} \text{tr}(\Gamma^* B (\Gamma^*)^\top) = \frac{d}{d\pi} \left(\frac{1}{c(\pi)} \right) \Big|_{\pi=0}. \quad (\text{SI.3.14})$$

Proof. The identity (SI.3.12) follows immediately from the block form of $G_e(\pi)$ in (SI.3.8) and the observation in (SI.3.11). To show (SI.3.14), we take the derivative of $1/c(\pi)$ with respect to π . From (SI.3.10), and using the identity

$$\frac{d}{d\pi} G(\pi) = -G(\pi) \Omega G(\pi),$$

we have

$$\begin{aligned} \frac{d}{d\pi} \left(\frac{1}{c(\pi)} \right) &= \frac{1}{d^3} \sum_{\mu, \nu \in [n]} y_\mu y_\nu \text{vec}(H_\mu)^\top G(\pi) \Omega G(\pi) \text{vec}(H_\nu) \\ &= q^\top(\pi) \Omega q(\pi). \end{aligned}$$

Thus, by (SI.3.11),

$$\begin{aligned} \frac{d}{d\pi} \left(\frac{1}{c(\pi)} \right) \Big|_{\pi=0} &= \frac{1}{d} (\text{vec}(\Gamma^*))^\top \Omega \text{vec}(\Gamma^*) \\ &= \frac{1}{d} (\text{vec}(\Gamma^*))^\top (I_d \otimes B) \text{vec}(\Gamma^*). \end{aligned}$$

Applying the identity in (SI.1.1) to the right-hand side of the above equation, we reach (SI.3.14). \square

Remark 3. To lighten the notation, we will often write $G_e(\pi)$ [resp. $G(\pi)$] as G_e [resp. G], leaving their dependence on the parameter π implicit.

Remark 4. In light of (SI.3.13) and (SI.3.14), we will always choose

$$\Omega = I_d \otimes B_{\text{test}}, \quad (\text{SI.3.15})$$

where B_{test} is the matrix defined in (SI.2.15).

SI.4 An Asymptotic Equivalent of the Extended Resolvent Matrix

In this section, we derive an asymptotic equivalent of the extended resolvent G_e defined in (SI.3.7). From this equivalent version, we can then obtain the asymptotic limits of the right-hand sides of (SI.3.12) and (SI.3.14). Our analysis relies on non-rigorous but technically sound heuristic arguments from random matrix theory. Therefore, we refer to our theoretical predictions as *results* rather than propositions.

Recall that there are k unique task vectors $\{w_i\}_{i \in [k]}$ in the training set. Let

$$b_{\text{tr}} := \frac{1}{k} \sum_{i \in [k]} w_i \quad \text{and} \quad R_{\text{tr}} := \frac{1}{k} \sum_{i \in [k]} w_i w_i^\top \quad (\text{SI.4.1})$$

denote the empirical mean and correlation matrix of these k regression vectors, respectively. Define

$$A_{\text{tr}} := \begin{bmatrix} R_{\text{tr}} & (1 + \rho)b_{\text{tr}} \end{bmatrix}. \quad (\text{SI.4.2})$$

and

$$E_{\text{tr}} := \begin{bmatrix} \frac{(1+\rho)}{\alpha} I_d + R_{\text{tr}} & (1 + \rho)b_{\text{tr}} \\ (1 + \rho)b_{\text{tr}}^\top & (1 + \rho)^2 \end{bmatrix}. \quad (\text{SI.4.3})$$

Definition 1. Consider the extended resolvent $G_e(\pi)$ in (SI.3.7), with Ω_e chosen in the forms of (SI.3.6) and (SI.3.15). Let \tilde{G}_e be another matrix of the same size as $G_e(\pi)$. We say that \tilde{G}_e and $G_e(\pi)$ are asymptotically equivalent, if the following conditions hold.

(1) For any two deterministic and unit-norm vectors $u, v \in \mathbb{R}^{d^2+d+1}$,

$$u^\top G_e(\pi)v \simeq u^\top \tilde{G}_e v, \quad (\text{SI.4.4})$$

where \simeq is the asymptotic equivalent notation defined in (SI.1.3).

(2) Let $A_{\text{tr}} = \begin{bmatrix} R_{\text{tr}} & (1 + \rho)b_{\text{tr}} \end{bmatrix}$. For any deterministic, unit-norm vector $v \in \mathbb{R}^{d^2+d+1}$,

$$\frac{1}{\sqrt{d}} \begin{bmatrix} 0 & \text{vec}(A_{\text{tr}})^\top \end{bmatrix} G_e(\pi)v \simeq \frac{1}{\sqrt{d}} \begin{bmatrix} 0 & \text{vec}(A_{\text{tr}})^\top \end{bmatrix} \tilde{G}_e v. \quad (\text{SI.4.5})$$

(3) Recall the notation introduced in (SI.1.2). We have

$$\frac{1}{d^2} \text{tr} \left([G_e(\pi)]_{\setminus 0} \cdot [I \otimes E_{\text{tr}}] \right) = \frac{1}{d^2} \text{tr} \left([\tilde{G}_e]_{\setminus 0} \cdot [I \otimes E_{\text{tr}}] \right) + \mathcal{O}_{\prec}(d^{-1/2}), \quad (\text{SI.4.6})$$

where $[G_e(\pi)]_{\setminus 0}$ and $[\mathcal{G}_e(\pi)]_{\setminus 0}$ denote the principal minors of $G_e(\pi)$ and $\mathcal{G}_e(\pi)$, respectively.

Result 3. Let χ_π denote the unique positive solution to the equation

$$\chi_\pi = \frac{1}{d} \text{tr} \left[\left(\frac{\tau}{1 + \chi_\pi} E_{\text{tr}} + \pi B_{\text{test}} + \lambda \tau I_d \right)^{-1} E_{\text{tr}} \right], \quad (\text{SI.4.7})$$

where B_{test} is the positive-semidefinite matrix in (SI.2.15), with $b_{\text{test}}, R_{\text{test}}$ chosen according to (SI.2.11) or (SI.2.12). The extended resolvent $G_e(\pi)$ in (SI.3.7) is asymptotically equivalent to

$$\mathcal{G}_e(\pi) := \left(\frac{\tau}{1 + \chi_\pi} \begin{bmatrix} 1 + \rho & \frac{1}{\sqrt{d}} \text{vec} \left(\begin{bmatrix} R_{\text{tr}} & (1 + \rho) b_{\text{tr}} \end{bmatrix} \right)^\top \\ \frac{1}{\sqrt{d}} \text{vec} \left(\begin{bmatrix} R_{\text{tr}} & (1 + \rho) b_{\text{tr}} \end{bmatrix} \right) & I_d \otimes E_{\text{tr}} \end{bmatrix} + \pi \Omega_e + \tau \lambda I \right)^{-1}, \quad (\text{SI.4.8})$$

in the sense of Definition 1. In the above expression, Ω_e is the matrix in (SI.3.6) with $\Omega = I_d \otimes B_{\text{test}}$.

In what follows, we present the steps in reaching the asymptotic equivalent $\mathcal{G}_e(\pi)$ given in (SI.4.8). To start, let $G_e^{[\mu]}$ to denote a ‘‘leave-one-out’’ version of G_e , defined as

$$G_e^{[\mu]} = \frac{1}{\sum_{\nu \neq \mu} z_\nu z_\nu^\top + \pi \Omega_e + \tau \lambda I}.$$

By (SI.3.7), we have

$$G_e \left(\sum_{\mu \in [n]} z_\mu z_\mu^\top + \pi \Omega_e + \tau \lambda I \right) = I.$$

Applying the Woodbury matrix identity then gives us

$$\sum_{\mu \in [n]} \frac{1}{1 + z_\mu^\top G_e^{[\mu]} z_\mu} G_e^{[\mu]} z_\mu z_\mu^\top + G_e(\pi \Omega_e + \tau \lambda I) = I. \quad (\text{SI.4.9})$$

To proceed, we study the quadratic form $z_\mu^\top G_e^{[\mu]} z_\mu$. Let w_μ denotes the task vector associated with z_μ . Conditioned on w_μ and G_e^μ , the quadratic form $z_\mu^\top G_e^{[\mu]} z_\mu$ concentrates around its *conditional expectation* with respect to the remaining randomness in z_μ . Specifically,

$$z_\mu^\top G_e^{[\mu]} z_\mu = \chi^\mu(w_\mu) + \mathcal{O}_{\prec}(d^{-1/2}),$$

where

$$\chi^\mu(w_\mu) := \frac{1}{d^2} \text{tr} \left([G_e^\mu]_{\setminus 0} \cdot [I \otimes E(w_\mu)] \right), \quad (\text{SI.4.10})$$

and

$$E(w) := \begin{bmatrix} \frac{1+\rho}{\alpha} I_d + w w^\top & (1 + \rho) w \\ (1 + \rho) w^\top & (1 + \rho)^2 \end{bmatrix}. \quad (\text{SI.4.11})$$

Substituting $z_\mu^\top G_e^{[\mu]} z_\mu$ in (SI.4.9) by $\chi^\mu(w_\mu)$, we get

$$\sum_{\mu \in [n]} \frac{1}{1 + \chi^\mu(w_\mu)} G_e^{[\mu]} z_\mu z_\mu^\top + G_e(\pi\Omega_e + \tau\lambda I) = I + \Delta_1, \quad (\text{SI.4.12})$$

where

$$\Delta_1 := \sum_{\mu \in [n]} \frac{z_\mu^\top G_e^{[\mu]} z_\mu - \chi^\mu(w_\mu)}{(1 + \chi^\mu(w_\mu))(1 + z_\mu^\top G_e^{[\mu]} z_\mu)} G_e^{[\mu]} z_\mu z_\mu^\top$$

is a matrix that captures the approximation error of the above substitution.

Next, we replace $z_\mu z_\mu^\top$ on the left-hand side of (SI.4.12) by its *conditional* expectation $\mathbb{E}_{w_\mu} [z_\mu z_\mu^\top]$, conditioned on the task vector w_μ . This allows us to rewrite (SI.4.12) as

$$\sum_{\mu \in [n]} \frac{1}{1 + \chi^\mu(w_\mu)} G_e^{[\mu]} \mathbb{E}_{w_\mu} [z_\mu z_\mu^\top] + G_e(\pi\Omega_e + \tau\lambda I) = I + \Delta_1 + \Delta_2, \quad (\text{SI.4.13})$$

where

$$\Delta_2 := \sum_{\mu \in [n]} \frac{1}{1 + \chi^\mu(w_\mu)} G_e^{[\mu]} \left(\mathbb{E}_{w_\mu} [z_\mu z_\mu^\top] - z_\mu z_\mu^\top \right)$$

captures the corresponding approximation error. Recall the definition of z_μ in (SI.3.5). Using the moment estimates in Lemma 1, we have

$$\mathbb{E}_{w_\mu} [z_\mu z_\mu^\top] = \frac{1}{d^2} \begin{bmatrix} 1 + \rho & \frac{1}{\sqrt{d}} w_\mu^\top \otimes \begin{bmatrix} w_\mu^\top & 1 + \rho \end{bmatrix} \\ \frac{1}{\sqrt{d}} w_\mu \otimes \begin{bmatrix} w_\mu \\ 1 + \rho \end{bmatrix} & I_d \otimes E(w_\mu) \end{bmatrix} + \frac{1}{d^2} \begin{bmatrix} 0 & \\ & I_d \otimes \mathcal{E}_\mu \end{bmatrix}, \quad (\text{SI.4.14})$$

where $E(w_\mu)$ is the matrix defined in (SI.4.11) and

$$\mathcal{E}_\mu = \frac{1}{\ell} \begin{bmatrix} w_\mu w_\mu^\top & 2(1 + \rho)w_\mu \\ 2(1 + \rho)w_\mu^\top & 2(1 + \rho)^2 \end{bmatrix}.$$

Replacing the conditional expectation $\mathbb{E}_{w_\mu} [z_\mu z_\mu^\top]$ in (SI.4.13) by the main (i.e. the first) term on the right-hand side of (SI.4.14), we can transform (SI.4.13) to

$$\frac{\tau}{n} \sum_{\mu \in [n]} \frac{1}{1 + \chi^\mu(w_\mu)} G_e^{[\mu]} \begin{bmatrix} 1 + \rho & \frac{1}{\sqrt{d}} w_\mu^\top \otimes \begin{bmatrix} w_\mu^\top & 1 + \rho \end{bmatrix} \\ \frac{1}{\sqrt{d}} w_\mu \otimes \begin{bmatrix} w_\mu \\ 1 + \rho \end{bmatrix} & I_d \otimes E(w_\mu) \end{bmatrix} + G_e(\pi\Omega_e + \tau\lambda I) = I + \Delta_1 + \Delta_2 + \Delta_3, \quad (\text{SI.4.15})$$

where we recall $\tau = n/d^2$, and we use Δ_3 to capture the approximation error associated with \mathcal{E}_μ .

Next, we replace the ‘‘leave-one-out’’ terms $G_e^{[\mu]}$ and $\chi^\mu(w_\mu)$ in (SI.4.15) by their ‘‘full’’ versions. Specifically, we replace $G_e^{[\mu]}$ by G_e , and $\chi^\mu(w_\mu)$ by

$$\chi(w_\mu) := \frac{1}{d^2} \text{tr} \left([G_e]_{\setminus 0} \cdot [I \otimes E(w_\mu)] \right). \quad (\text{SI.4.16})$$

It is important to note the difference between (SI.4.10) and (SI.4.16): the former uses G_e^μ and the latter G_e . After these replacements and using Δ_4 to capture the approximation errors, we have

$$G_e \left(\frac{\tau}{n} \sum_{\mu \in [n]} \frac{1}{1 + \chi(w_\mu)} \begin{bmatrix} 1 + \rho & \frac{1}{\sqrt{d}} w_\mu^\top \otimes \begin{bmatrix} w_\mu^\top & 1 + \rho \end{bmatrix} \\ \frac{1}{\sqrt{d}} w_\mu \otimes \begin{bmatrix} w_\mu \\ 1 + \rho \end{bmatrix} & I_d \otimes E(w_\mu) \end{bmatrix} + \pi \Omega_e + \tau \lambda I \right) = I + \sum_{j \leq 4} \Delta_j. \quad (\text{SI.4.17})$$

Recall that there are k unique task vectors $\{w_i\}_{1 \leq i \leq k}$ in the training set consisting of n input samples. Each sample is associated with one of these task vectors, sampled uniformly from the set $\{w_i\}_{1 \leq i \leq k}$. In our analysis, we shall assume that k divides n and that each unique task vector is associated with exactly n/k input samples. (We note that this assumption merely serves to simplify the notation. The asymptotic characterization of the random matrix G_e remains the same even without this assumption.) Observe that there are only k unique terms in the sum on the left-hand side of (SI.4.17). Thus,

$$G_e \left(\frac{\tau}{k} \sum_{i \in [k]} \frac{1}{1 + \chi(w_i)} \begin{bmatrix} 1 + \rho & \frac{1}{\sqrt{d}} w_i^\top \otimes \begin{bmatrix} w_i^\top & 1 + \rho \end{bmatrix} \\ \frac{1}{\sqrt{d}} w_i \otimes \begin{bmatrix} w_i \\ 1 + \rho \end{bmatrix} & I_d \otimes E(w_i) \end{bmatrix} + \pi \Omega_e + \tau \lambda I \right) = I + \sum_{j \leq 4} \Delta_j. \quad (\text{SI.4.18})$$

So far, we have been treating the k task vectors $\{w_i\}_{i \in [k]}$ as fixed vectors, only using the randomness in the input samples that are associated with the data vectors $\{x_i^\mu\}$. To further simplify our asymptotic characterization, we take advantage of the fact that $\{w_i\}_{i \in [k]}$ are independently sampled from $\text{Unif}(\mathcal{S}^{d-1}(\sqrt{d}))$. To that end, we can first show that $\chi(w_i)$ in (SI.4.16) concentrates around its expectation. Specifically,

$$\chi(w_i) = \mathbb{E} \left[\frac{1}{d^2} \text{tr} \left([G_e]_{\setminus 0} \cdot [I \otimes E(w_i)] \right) \right] + \mathcal{O}_{\prec}(d^{-1/2}).$$

By symmetry, we must have

$$\mathbb{E} \left[\frac{1}{d^2} \text{tr} \left([G_e]_{\setminus 0} \cdot [I \otimes E(w_i)] \right) \right] = \mathbb{E} \left[\frac{1}{d^2} \text{tr} \left([G_e]_{\setminus 0} \cdot [I \otimes E(w_j)] \right) \right]$$

for any $1 \leq i < j \leq k$. It follows that $|\chi(w_i) - \chi(w_j)| = \mathcal{O}_{\prec}(d^{-1/2})$, and thus, by a union bound,

$$\max_{i \in [k]} |\chi(w_{k_1}) - \widehat{\chi}_{\text{ave}}| = \mathcal{O}_{\prec}(d^{-1/2}), \quad (\text{SI.4.19})$$

where

$$\widehat{\chi}_{\text{ave}} := \frac{1}{k} \sum_{i \in [k]} \chi(w_i). \quad (\text{SI.4.20})$$

Upon substituting (SI.4.16) into (SI.4.20), it is straightforward to verify the following characterization of $\widehat{\chi}_{\text{ave}}$:

$$\widehat{\chi}_{\text{ave}} = \frac{1}{d^2} \text{tr} \left([G_e]_{\setminus 0} \cdot [I \otimes E_{\text{tr}}] \right). \quad (\text{SI.4.21})$$

The estimate in (SI.4.19) prompts us to replace the terms $\chi(w_i)$ in the right-hand side of (SI.4.18) by the common value $\widehat{\chi}_{\text{ave}}$. As before, we introduce a matrix Δ_5 to capture the approximation error

associated with this step. Using the newly introduced notation $E_{\text{tr}}, b_{\text{tr}}$ and R_{tr} in (SI.4.3) and (SI.4.1), we can then simplify (SI.4.18) as

$$G_e \left(\frac{\tau}{1 + \widehat{\chi}_{\text{ave}}} \begin{bmatrix} 1 + \rho & \frac{1}{\sqrt{d}} \text{vec} \left(\left[R_{\text{tr}} \quad (1 + \rho) b_{\text{tr}} \right] \right)^\top \\ \frac{1}{\sqrt{d}} \text{vec} \left(\left[R_{\text{tr}} \quad (1 + \rho) b_{\text{tr}} \right] \right) & I_d \otimes E_{\text{tr}} \end{bmatrix} + \pi \Omega_e + \tau \lambda I \right) \\ = I + \sum_{1 \leq j \leq 5} \Delta_j.$$

Define

$$\widehat{\mathcal{G}}_e(\pi) := \left(\frac{\tau}{1 + \widehat{\chi}_{\text{ave}}} \begin{bmatrix} 1 + \rho & \frac{1}{\sqrt{d}} \text{vec} \left(\left[R_{\text{tr}} \quad (1 + \rho) b_{\text{tr}} \right] \right)^\top \\ \frac{1}{\sqrt{d}} \text{vec} \left(\left[R_{\text{tr}} \quad (1 + \rho) b_{\text{tr}} \right] \right) & I_d \otimes E_{\text{tr}} \end{bmatrix} + \pi \Omega_e + \tau \lambda I \right)^{-1}. \quad (\text{SI.4.22})$$

Then

$$G_e = \widehat{\mathcal{G}}_e(\pi) + \underbrace{\widehat{\mathcal{G}}_e(\pi) (\Delta_1 + \Delta_2 + \Delta_3 + \Delta_4 + \Delta_5)}_{\text{approximation errors}}. \quad (\text{SI.4.23})$$

Remark 5. We claim that $\widehat{\mathcal{G}}_e$ is asymptotically equivalent to G_e , in the sense of Definition 1. Given (SI.4.23), proving this claim requires showing that, for $j = 1, 2, \dots, 5$,

$$u^\top \left(\widehat{\mathcal{G}}_e(\pi) \Delta_j \right) v \simeq 0,$$

$$\frac{1}{\sqrt{d}} \begin{bmatrix} 0 & \text{vec}(A_{\text{tr}})^\top \end{bmatrix} \left(\widehat{\mathcal{G}}_e(\pi) \Delta_j \right) v \simeq 0,$$

and

$$\frac{1}{d^2} \text{tr} \left(\left[\widehat{\mathcal{G}}_e(\pi) \Delta_j \right]_{\setminus 0} \cdot [I \otimes E_{\text{tr}}] \right) \simeq 0,$$

for any deterministic and unit-norm vectors u, v and for $A_{\text{tr}} = \begin{bmatrix} R_{\text{tr}} & (1 + \rho) b_{\text{tr}} \end{bmatrix}$.

We note the equivalent matrix $\widehat{\mathcal{G}}_e(\pi)$ still involves one scalar $\widehat{\chi}_{\text{ave}}$ that depends on the original resolvent $G_e(\pi)$. Next, we show that $\widehat{\chi}_{\text{ave}}$ can be replaced by χ_π , the unique positive solution to (SI.4.7). To that end, we recall the characterization in (SI.4.21). Using the claim that $G_e(\pi)$ and $\widehat{\mathcal{G}}_e(\pi)$ are asymptotically equivalent (in particular, in the sense of (SI.4.6)), we have

$$\widehat{\chi}_{\text{ave}} \simeq \frac{1}{d^2} \text{tr} \left(\left[\widehat{\mathcal{G}}_e(\pi) \right]_{\setminus 0} \cdot [I \otimes E_{\text{tr}}] \right). \quad (\text{SI.4.25})$$

To compute the first term on the right-hand side of the above estimate, we directly invert the block matrix $\widehat{\mathcal{G}}_e(\pi)$ in (SI.4.22). Recall that Ω_e is chosen in the forms of (SI.3.6) and (SI.3.13). It is then straightforward to verify that

$$\widehat{\mathcal{G}}_e = \begin{bmatrix} \bar{c} & -\bar{c} \bar{q}^\top \\ -\bar{c} \bar{q} & I \otimes F_E(\widehat{\chi}_{\text{ave}}) + \bar{c} \bar{q} \bar{q}^\top \end{bmatrix}, \quad (\text{SI.4.26})$$

where $F_E(\chi)$ is a matrix valued function such that

$$F_E(\chi) = \left(\frac{\tau}{1+\chi} E_{\text{tr}} + \pi B + \lambda \tau I_{d+1} \right)^{-1}, \quad (\text{SI.4.27})$$

$$\bar{q} = \frac{\tau}{(1+\hat{\chi}_{\text{ave}})\sqrt{d}} \text{vec} \left(\begin{bmatrix} R_{\text{tr}} & (1+\rho)b_{\text{tr}} \end{bmatrix} F_E(\hat{\chi}_{\text{ave}}) \right),$$

and

$$1/\bar{c} = \frac{\tau(1+\rho)}{1+\hat{\chi}_{\text{ave}}} + \lambda\tau - \frac{\tau^2}{(1+\hat{\chi}_{\text{ave}})^2 d} \text{tr} \left(\begin{bmatrix} R_{\text{tr}} & (1+\rho)b_{\text{tr}} \end{bmatrix} F_E(\hat{\chi}_{\text{ave}}) \begin{bmatrix} R_{\text{tr}} & (1+\rho)b_{\text{tr}} \end{bmatrix}^\top \right).$$

Using (SI.4.26), we can now write the equation (SI.4.25) as

$$\begin{aligned} \hat{\chi}_{\text{ave}} &\simeq \frac{1}{d} \text{tr} (F_E(\hat{\chi}_{\text{ave}}) E_{\text{tr}}) \\ &+ \frac{\bar{c} \tau^2}{(1+\hat{\chi}_{\text{ave}})^2 d^3} \text{tr} \left(\begin{bmatrix} R_{\text{tr}} & (1+\rho)b_{\text{tr}} \end{bmatrix} F_E(\hat{\chi}_{\text{ave}}) E_{\text{tr}} F_E(\hat{\chi}_{\text{ave}}) \begin{bmatrix} R_{\text{tr}} & (1+\rho)b_{\text{tr}} \end{bmatrix}^\top \right). \end{aligned} \quad (\text{SI.4.28})$$

The second term on the right-hand side of (SI.4.28) is negligible. Indeed,

$$\begin{aligned} &\text{tr} \left(\begin{bmatrix} R_{\text{tr}} & (1+\rho)b_{\text{tr}} \end{bmatrix} F_E(\hat{\chi}_{\text{ave}}) E_{\text{tr}} F_E(\hat{\chi}_{\text{ave}}) \begin{bmatrix} R_{\text{tr}} & (1+\rho)b_{\text{tr}} \end{bmatrix}^\top \right) \\ &\leq \|F_E(\hat{\chi}_{\text{ave}}) E_{\text{tr}} F_E(\hat{\chi}_{\text{ave}})\|_{\text{op}} (\|R_{\text{tr}}\|_{\text{F}}^2 + (1+\rho)^2 \|b_{\text{tr}}\|^2). \end{aligned}$$

By construction, $\|F_E(\hat{\chi}_{\text{ave}})\|_{\text{op}} \leq (\lambda\tau)^{-1}$. Moreover, since the task vectors $\{w_i\}_{i \in [k]}$ are independent vectors sampled from $\text{Unif}(\mathcal{S}^{d-1}(\sqrt{d}))$, it is easy to verify that

$$\|E_{\text{tr}}\|_{\text{op}} = \mathcal{O}_{\prec}(1), \quad \|R_{\text{tr}}\|_{\text{F}} = \mathcal{O}_{\prec}(\sqrt{d}) \quad \text{and} \quad \|b_{\text{tr}}\|_2 = \mathcal{O}_{\prec}(1).$$

Finally, since \bar{c} is an element of $\hat{\mathcal{G}}_e$, we must have $|\bar{c}| \leq \|\hat{\mathcal{G}}_e\|_{\text{op}} \leq (\tau\lambda)^{-1}$. Combining these estimates gives us

$$\frac{\bar{c} \tau^2}{(1+\hat{\chi}_{\text{ave}})^2 d^3} \text{tr} \left(\begin{bmatrix} R_{\text{tr}} & (1+\rho)b_{\text{tr}} \end{bmatrix} F_E(\hat{\chi}_{\text{ave}}) E_{\text{tr}} F_E(\hat{\chi}_{\text{ave}}) \begin{bmatrix} R_{\text{tr}} & (1+\rho)b_{\text{tr}} \end{bmatrix}^\top \right) = \mathcal{O}_{\prec}(d^{-2}),$$

and thus we can simplify (SI.4.28) as

$$\hat{\chi}_{\text{ave}} \simeq \frac{1}{d} \text{tr} \left[\left(\frac{\tau}{1+\hat{\chi}_{\text{ave}}} E_{\text{tr}} + \pi B + \lambda \tau I_d \right)^{-1} E_{\text{tr}} \right]. \quad (\text{SI.4.29})$$

Observe that (SI.4.29) is a small perturbation of the self-consistent equation in (SI.4.7). By the stability of the equation (SI.4.7), we then have

$$\hat{\chi}_{\text{ave}} \simeq \chi_\pi, \quad (\text{SI.4.30})$$

where χ_π is the unique positive solution to (SI.4.7).

Recall the definitions of $\mathcal{G}_e(\pi)$ and $\widehat{\mathcal{G}}_e(\pi)$ in (SI.4.22) and (SI.4.8), respectively. By the standard resolvent identity,

$$\begin{aligned} & \widehat{\mathcal{G}}_e(\pi) - \mathcal{G}_e(\pi) \\ &= \frac{\tau[\widehat{\chi}_{\text{ave}} - \chi\pi]}{[1 + \chi\pi][1 + \widehat{\chi}_{\text{ave}}]} \widehat{\mathcal{G}}_e(\pi) \begin{bmatrix} 1 + \rho & \frac{1}{\sqrt{d}} \text{vec} \left(\begin{bmatrix} R_{\text{tr}} & (1 + \rho)b_{\text{tr}} \end{bmatrix} \right)^\top \\ \frac{1}{\sqrt{d}} \text{vec} \left(\begin{bmatrix} R_{\text{tr}} & (1 + \rho)b_{\text{tr}} \end{bmatrix} \right) & I_d \otimes E_{\text{tr}} \end{bmatrix} \mathcal{G}_e(\pi). \end{aligned} \quad (\text{SI.4.31})$$

By construction, $\|\widehat{\mathcal{G}}_e(\pi)\|_{\text{op}} \leq 1/(\tau\lambda)$ and $\|\mathcal{G}_e(\pi)\|_{\text{op}} \leq 1/(\tau\lambda)$. Moreover, $\|E_{\text{tr}}\|_{\text{op}} \prec 1$ and

$$\left\| \frac{1}{\sqrt{d}} \text{vec} \left(\begin{bmatrix} R_{\text{tr}} & (1 + \rho)b_{\text{tr}} \end{bmatrix} \right) \right\| \prec 1.$$

It then follows from (SI.4.30) and (SI.4.31) that

$$\left\| \widehat{\mathcal{G}}_e(\pi) - \mathcal{G}_e(\pi) \right\|_{\text{op}} \simeq 0. \quad (\text{SI.4.32})$$

If $\widehat{\mathcal{G}}_e(\pi)$ satisfies the equivalent conditions (SI.4.4), (SI.4.5) and (SI.4.6) (as claimed in our analysis above), then the estimate in (SI.4.32) allows us to easily check that $\mathcal{G}_e(\pi)$ also satisfies (SI.4.4), (SI.4.5) and (SI.4.6). Thus, we claim that $\mathcal{G}_e(\pi)$ is asymptotically equivalent to the extended resolvent matrix $G_e(\pi)$ in the sense of Definition 1.

SI.5 Asymptotic Limits of the Generalization Errors

In this section, we use the characterization in Result 3 to derive the asymptotic limits of the generalization errors of associated with the set of parameters Γ^* learned from ridge regression.

SI.5.1 Asymptotic Limits of the Linear and Quadratic Terms

From Corollary 1 and the discussions in Remark 2, characterizing the test error $e(\Gamma^*)$ boils down to computing the linear term $\frac{1}{d} \text{tr} \left(\Gamma^* A_{\text{test}}^\top \right)$ and the quadratic term $\frac{1}{d} \text{tr} \left(\Gamma^* B_{\text{test}} (\Gamma^*)^\top \right)$, where A_{test} and B_{test} are the matrices defined in (SI.2.14) and (SI.2.15), respectively.

We consider two different types of test data distributions $\mathcal{P}_{\text{test}}$: ICL and IDG. [See Section 2.6 in the main text for details.] From (SI.2.11) and (SI.2.12), these two settings correspond to choosing

$$(\text{ICL}) : \quad A_{\text{test}} = \begin{bmatrix} I_d & 0 \end{bmatrix} \quad \text{and} \quad B_{\text{test}} = \begin{bmatrix} \left(\frac{1+\rho}{\alpha} + 1 \right) I_d & \\ & (1 + \rho)^2 \end{bmatrix}. \quad (\text{SI.5.1})$$

and

$$(\text{IDG}) : \quad A_{\text{test}} = A_{\text{tr}} \quad \text{and} \quad B_{\text{test}} = E_{\text{tr}}, \quad (\text{SI.5.2})$$

respectively. In (SI.5.2), A_{tr} and E_{tr} are the matrices defined in (SI.4.2) and (SI.4.3).

Result 4. *Let Γ^* be the set of parameters learned from the ridge regression problem in (9). Let $A_{\text{test}} \in \mathbb{R}^{d \times (d+1)}$ and $B_{\text{test}} \in \mathbb{R}^{(d+1) \times (d+1)}$ be two matrices constructed as in (SI.5.1) or (SI.5.2). We have*

$$\frac{1}{d} \text{tr}(\Gamma^* A_{\text{test}}^\top) \simeq \frac{1}{d} \text{tr} \left(\Gamma_{\text{eq}}^* A_{\text{test}}^\top \right), \quad (\text{SI.5.3})$$

and

$$\frac{1}{d} \operatorname{tr}(\Gamma^* B_{\text{test}} (\Gamma^*)^\top) \simeq \frac{1}{d} \operatorname{tr}(\Gamma_{\text{eq}}^* B_{\text{test}} (\Gamma_{\text{eq}}^*)^\top) - \frac{c_e}{d} \operatorname{tr} \left(B_{\text{test}} \left[(E_{\text{tr}} + \xi I)^{-1} - \xi (E_{\text{tr}} + \xi I)^{-2} \right] \right). \quad (\text{SI.5.4})$$

In the above displays, Γ_{eq}^* is an asymptotic equivalent of Γ^* , defined as

$$\Gamma_{\text{eq}}^* := \begin{bmatrix} R_{\text{tr}} & (1 + \rho) b_{\text{tr}} \end{bmatrix} (E_{\text{tr}} + \xi I)^{-1}, \quad (\text{SI.5.5})$$

where ξ is the unique positive solution to the self-consistent equation

$$\xi \mathcal{M}_\kappa \left(\frac{1 + \rho}{\alpha} + \xi \right) - \frac{\tau \lambda}{\xi} = 1 - \tau, \quad (\text{SI.5.6})$$

and $\mathcal{M}_\kappa(\cdot)$ is the function defined in (B.3). Moreover, the scalar c_e in (SI.5.4) is defined as

$$c_e = \frac{\rho + \nu - \nu^2 \mathcal{M}_\kappa(\nu) - \xi [1 - 2\nu \mathcal{M}_\kappa(\nu) - \nu^2 \mathcal{M}'_\kappa(\nu)]}{1 - 2\xi \mathcal{M}_\kappa(\nu) - \xi^2 \mathcal{M}'_\kappa(\nu) - \tau}, \quad (\text{SI.5.7})$$

where

$$\nu := \frac{1 + \rho}{\alpha} + \xi. \quad (\text{SI.5.8})$$

To derive the asymptotic characterizations (SI.5.3) and (SI.5.4) in Result 4, we first use block-matrix inversion to rewrite $\mathcal{G}_e(\pi)$ in (SI.4.8) as

$$\mathcal{G}_e(\pi) = \begin{bmatrix} c^*(\pi) & -c^*(\pi) (q^*(\pi))^\top \\ -c^*(\pi) q^*(\pi) & I \otimes F_E(\chi_\pi) + c^*(\pi) q^*(\pi) (q^*(\pi))^\top \end{bmatrix}, \quad (\text{SI.5.9})$$

where $F_E(\cdot)$ is the matrix-valued function defined in (SI.4.27), *i.e.*,

$$F_E(\chi_\pi) = \left(\frac{\tau}{1 + \chi_\pi} E_{\text{tr}} + \pi B_{\text{test}} + \lambda \tau I_{d+1} \right)^{-1}.$$

Moreover,

$$q^*(\pi) = \frac{\tau}{(1 + \chi_\pi) \sqrt{d}} \operatorname{vec} \left(\begin{bmatrix} R_{\text{tr}} & (1 + \rho) b_{\text{tr}} \end{bmatrix} F_E(\chi_\pi) \right), \quad (\text{SI.5.10})$$

and

$$\frac{1}{c^*(\pi)} = \frac{\tau(1 + \rho)}{1 + \chi_\pi} + \lambda \tau - \frac{\tau^2}{(1 + \chi_\pi)^2 d} \operatorname{tr} \left(\begin{bmatrix} R_{\text{tr}} & (1 + \rho) b_{\text{tr}} \end{bmatrix} F_E(\chi_\pi) \begin{bmatrix} R_{\text{tr}} & (1 + \rho) b_{\text{tr}} \end{bmatrix}^\top \right). \quad (\text{SI.5.11})$$

Observe that there is a one-to-one correspondence between the terms in (SI.5.9) and those in (SI.3.8).

To derive the asymptotic characterization given in (SI.5.3), we note that

$$\frac{1}{d} \operatorname{tr}(\Gamma^* A_{\text{test}}^\top) \simeq \frac{-1}{c(0) \sqrt{d}} \begin{bmatrix} 0 & \operatorname{vec}(A_{\text{test}})^\top \end{bmatrix} \mathcal{G}_e(0) e_1 \quad (\text{SI.5.12})$$

$$= \frac{c^*(0)}{c(0)} \cdot \frac{1}{d} \operatorname{tr} \left(\begin{bmatrix} R_{\text{tr}} & (1 + \rho) b_{\text{tr}} \end{bmatrix} (E_{\text{tr}} + \lambda(1 + \chi_0) I)^{-1} A_{\text{test}}^\top \right) \quad (\text{SI.5.13})$$

$$\simeq \frac{1}{d} \operatorname{tr} \left(\begin{bmatrix} R_{\text{tr}} & (1 + \rho) b_{\text{tr}} \end{bmatrix} (E_{\text{tr}} + \lambda(1 + \chi_0) I)^{-1} A_{\text{test}}^\top \right). \quad (\text{SI.5.14})$$

In the above display, (SI.5.12) follows from (SI.3.12) and the asymptotic equivalence between $G_e(0)$ and $\mathcal{G}_e(0)$. The equality in (SI.5.13) is due to (SI.5.9) and (SI.5.10). To reach (SI.5.14), we note that $c(0) = e_1^\top G_e(0)e_1$ and $c^*(0) = e_1^\top \mathcal{G}_e(0)e_1$. Thus, $c(0) \simeq c^*(0)$ due to the asymptotic equivalence between $G_e(0)$ and $\mathcal{G}_e(0)$. In Appendix B, we show that

$$\lambda(1 + \chi_0) \simeq \xi, \quad (\text{SI.5.15})$$

where ξ is the scalar defined in (SI.5.6). The asymptotic characterization given in (SI.5.3) then follows from (SI.5.14) and from the definition of Γ_{eq}^* given in (SI.5.5).

Next, we use (SI.3.14) to derive the asymptotic characterization of the quadratic term in (SI.5.4). Taking the derivative of (SI.5.11) gives us

$$\begin{aligned} \frac{d}{d\pi} \left(\frac{1}{c^*(\pi)} \right) \Big|_{\pi=0} &= \frac{1}{d} \text{tr}(\Gamma_{\text{eq}}^* B_{\text{test}}(\Gamma_{\text{eq}}^*)^\top) \\ &\quad - \frac{\tau\chi'_0}{(1 + \chi_0)^2} \left(1 + \rho - \frac{2}{d} \text{tr}(A_{\text{tr}}(E_{\text{tr}} + \xi I)^{-1} A_{\text{tr}}^\top) + \frac{1}{d} \text{tr}(A_{\text{tr}}(E_{\text{tr}} + \xi I)^{-1} E_{\text{tr}}(E_{\text{tr}} + \xi I)^{-1} A_{\text{tr}}^\top) \right) \\ &= \frac{1}{d} \text{tr}(\Gamma_{\text{eq}}^* B_{\text{test}}(\Gamma_{\text{eq}}^*)^\top) - \frac{\tau\chi'_0}{(1 + \chi_0)^2} \left(1 + \rho - \frac{1}{d} \text{tr}(\Gamma_{\text{eq}}^* A_{\text{tr}}^\top) - \frac{\xi}{d} \text{tr}(\Gamma_{\text{eq}}^* (\Gamma_{\text{eq}}^*)^\top) \right), \end{aligned} \quad (\text{SI.5.16})$$

where A_{tr} is the matrix defined in (SI.4.2). In reaching the above expression, we have also used the estimate in (SI.5.15).

To further simplify our formula, we note that

$$A_{\text{tr}} = S \left(E_{\text{tr}} + \xi I_{d+1} - \left(\frac{1 + \rho}{\alpha} + \xi \right) I_{d+1} \right), \quad (\text{SI.5.17})$$

where S is a $d \times (d + 1)$ matrix obtained by removing the last row of I_{d+1} . Using this identity, we can rewrite the matrix Γ_{eq}^* in (SI.5.5) as

$$\Gamma_{\text{eq}}^* = S \left(I - \left(\frac{1 + \rho}{\alpha} + \xi \right) (E_{\text{tr}} + \xi I)^{-1} \right) \quad (\text{SI.5.18})$$

$$= \begin{bmatrix} I - \nu F_R(\nu) - a^*(1 + \rho)^2 \nu F_R(\nu) b_{\text{tr}} b_{\text{tr}}^\top F_R(\nu) & a^*(1 + \rho) \nu F_R(\nu) b_{\text{tr}} \end{bmatrix}, \quad (\text{SI.5.19})$$

where $F_R(\cdot)$ is the function defined in (B.1), and ν is the parameter given in (SI.5.8). The second equality (SI.5.19) is obtained from the explicit formula for $(E_{\text{tr}} + \xi I)^{-1}$ in (B.6).

From (SI.5.17) and (SI.5.18), it is straightforward to check that

$$\frac{1}{d} \text{tr}(\Gamma_{\text{eq}}^* A_{\text{tr}}^\top) = 1 - \nu + \nu^2 \frac{1}{d} \text{tr}(S(E_{\text{tr}} + \xi I)^{-1} S^\top),$$

and

$$\frac{\xi}{d} \text{tr}(\Gamma_{\text{eq}}^* (\Gamma_{\text{eq}}^*)^\top) = \xi \left[1 - 2\nu \frac{1}{d} \text{tr}(S(E_{\text{tr}} + \xi I)^{-1} S^\top) + \nu^2 \frac{1}{d} \text{tr}(S(E_{\text{tr}} + \xi I)^{-2} S^\top) \right].$$

By using the asymptotic characterizations given in (B.15) and (B.16), we then have

$$\frac{1}{d} \text{tr}(\Gamma_{\text{eq}}^* A_{\text{tr}}^\top) \simeq 1 - \nu + \nu^2 \mathcal{M}_\kappa(\nu), \quad (\text{SI.5.20})$$

and

$$\frac{\xi}{d} \text{tr}(\Gamma_{\text{eq}}^* (\Gamma_{\text{eq}}^*)^\top) \simeq \xi \left[1 - 2\nu \mathcal{M}_\kappa(\nu) - \nu^2 \mathcal{M}'_\kappa(\nu) \right]. \quad (\text{SI.5.21})$$

Substituting (SI.5.20), (SI.5.21), and (B.17) into (SI.5.16) yields

$$\frac{d}{d\pi} \left(\frac{1}{c^*(\pi)} \right) \Big|_{\pi=0} \simeq \frac{1}{d} \text{tr}(\Gamma_{\text{eq}}^* B_{\text{test}} (\Gamma_{\text{eq}}^*)^T) - \frac{c_e}{d} \text{tr} \left(B_{\text{test}} \left[(E_{\text{tr}} + \xi I)^{-1} - \xi (E_{\text{tr}} + \xi I)^{-2} \right] \right),$$

where c_e is the scalar defined in (SI.5.7). The asymptotic characterization of the quadratic term in (SI.5.4) then follows from (SI.3.14) and the claim that

$$\frac{d}{d\pi} \left(\frac{1}{c(\pi)} \right) \Big|_{\pi=0} \simeq \frac{d}{d\pi} \left(\frac{1}{c^*(\pi)} \right) \Big|_{\pi=0}.$$

SI.5.2 The Generalization Error of In-Context Learning

Result 5. Consider the test distribution $\mathcal{P}_{\text{test}}$ associated with the ICL task. We have

$$e(\Gamma^*) \simeq e^{\text{ICL}}(\tau, \alpha, \kappa, \rho, \lambda), \quad (\text{SI.5.22})$$

where

$$\begin{aligned} e^{\text{ICL}}(\tau, \alpha, \kappa, \rho, \lambda) := & \left(\frac{1+\rho}{\alpha} + 1 \right) \left(1 - 2\nu \mathcal{M}_\kappa(\nu) - \nu^2 \mathcal{M}'_\kappa(\nu) - c_e [\mathcal{M}_\kappa(\nu) + \xi \mathcal{M}'_\kappa(\nu)] \right) \\ & - 2 [1 - \nu \mathcal{M}_\kappa(\nu)] + 1 + \rho, \end{aligned}$$

and c_e is the constant given in (SI.5.7).

Remark 6. Recall the definition of the asymptotic equivalence notation “ \simeq ” introduced in Section SI.1. The characterization given in (SI.5.22) implies that, as $d \rightarrow \infty$, the generalization error $e(\Gamma^*)$ converges almost surely to the deterministic quantity $e^{\text{ICL}}(\tau, \alpha, \kappa, \rho, \lambda)$.

To derive (SI.5.22), our starting point is the estimate

$$e(\Gamma^*) \simeq \frac{1}{d} \text{tr} \left(\Gamma^* B_{\text{test}} (\Gamma^*)^\top \right) - \frac{2}{d} \text{tr} \left(\Gamma^* A_{\text{test}}^\top \right) + 1 + \rho, \quad (\text{SI.5.23})$$

which follows from Corollary 1 and the discussions in Remark 2. We consider the ICL task here, and thus A_{test} and B_{test} are given in (SI.5.1). The asymptotic limits of the first two terms on the right-hand side of the above equation can be obtained by the characterizations given in Result 4.

Using (SI.5.3) and the expressions in (SI.5.19) and (SI.5.1), we have

$$\begin{aligned} \frac{1}{d} \text{tr}(\Gamma^* A_{\text{test}}^\top) & \simeq \frac{1}{d} \text{tr} \left(\Gamma_{\text{eq}}^* A_{\text{test}}^\top \right) \\ & = 1 - \frac{\nu}{d} \text{tr} F_R(\nu) - a^*(1+\rho)^2 \nu \frac{\|F_R(\nu) b_{\text{tr}}\|^2}{d} \\ & \simeq 1 - \nu \mathcal{M}_\kappa(\nu), \end{aligned} \quad (\text{SI.5.24})$$

where ν is the constant defined in (SI.5.8). To reach the last step, we have used the estimate given in (B.15).

Next, we use (SI.5.4) to characterize the first term on the right-hand side of (SI.5.23). From the formulas in (SI.5.19) and (SI.5.1), we can check that

$$\begin{aligned} \frac{1}{d} \text{tr} \left(\Gamma_{\text{eq}}^* B_{\text{test}} (\Gamma_{\text{eq}}^*)^\top \right) & \simeq \left(\frac{1+\rho}{\alpha} + 1 \right) \frac{1}{d} \text{tr} (I - \nu F(\nu))^2 \\ & \simeq \left(\frac{1+\rho}{\alpha} + 1 \right) \left(1 - 2\nu \mathcal{M}_\kappa(\nu) - \nu^2 \mathcal{M}'_\kappa(\nu) \right), \end{aligned} \quad (\text{SI.5.25})$$

where the second step follows from (B.15) and (B.16). From (B.6),

$$\frac{1}{d} \operatorname{tr}(B_{\text{test}}(E_{\text{tr}} + \xi I)^{-1}) \simeq \left(\frac{1+\rho}{\alpha} + 1 \right) \frac{1}{d} \operatorname{tr} F_R(\nu) \simeq \left(\frac{1+\rho}{\alpha} + 1 \right) \mathcal{M}_\kappa(\nu). \quad (\text{SI.5.26})$$

Similarly, we can check that

$$\frac{1}{d} \operatorname{tr}(B_{\text{test}}(E_{\text{tr}} + \xi I)^{-2}) \simeq \left(\frac{1+\rho}{\alpha} + 1 \right) \frac{1}{d} \operatorname{tr} F_R^2(\nu) \simeq - \left(\frac{1+\rho}{\alpha} + 1 \right) \mathcal{M}'_\kappa(\nu). \quad (\text{SI.5.27})$$

Substituting (SI.5.25), (SI.5.26), and (SI.5.27) into (SI.5.4) gives us

$$\frac{1}{d} \operatorname{tr}(\Gamma^* B(\Gamma^*)^\top) \simeq \left(\frac{1+\rho}{\alpha} + 1 \right) \left(1 - 2\nu \mathcal{M}_\kappa(\nu) - \nu^2 \mathcal{M}'_\kappa(\nu) - c_e [\mathcal{M}_\kappa(\nu) + \xi \mathcal{M}'_\kappa(\nu)] \right), \quad (\text{SI.5.28})$$

where c_e is the constant given in (SI.5.7). Combining (SI.5.24), (SI.5.28), and (SI.5.23), we are done.

In what follows, we further simplify the characterizations in Result 5 by considering the ridgeless limit, *i.e.*, when $\lambda \rightarrow 0^+$.

Result 6. *Let*

$$q^* := \frac{1+\rho}{\alpha}, \quad m^* := \mathcal{M}_\kappa(q^*), \quad \text{and} \quad \mu^* := q^* \mathcal{M}_{\kappa/\tau}(q^*), \quad (\text{SI.5.29})$$

where $\mathcal{M}_\kappa(x)$ is the function defined in (B.3). Then

$$e_{\text{ridgeless}}^{\text{ICL}} := \lim_{\lambda \rightarrow 0^+} e^{\text{ICL}}(\tau, \alpha, \kappa, \rho, \lambda) = \begin{cases} \frac{\tau(1+q^*)}{1-\tau} [1 - \tau(1 - \mu^*)^2 + \mu^*(\rho/q^* - 1)] - 2\tau(1 - \mu^*) + (1 + \rho) & \tau < 1 \\ (q^* + 1) \left(1 - 2q^*m^* - (q^*)^2 \mathcal{M}'_\kappa(q^*) + \frac{(\rho+q^*-(q^*)^2 m^*)m^*}{\tau-1} \right) - 2(1 - q^*m^*) + (1 + \rho) & \tau > 1 \end{cases}, \quad (\text{SI.5.30})$$

where $\mathcal{M}'_\kappa(\cdot)$ denotes the derivative of $\mathcal{M}_\kappa(x)$ with respect to x .

We start with the case of $\tau < 1$. Examining the self-consistent equation in (SI.5.6), we can see that the parameter ξ tends to a nonzero constant, denoted by ξ^* , as $\lambda \rightarrow 0^+$. It follows that the original equation in (SI.5.6) reduces to

$$\xi^* \mathcal{M}_\kappa \left(\frac{1+\rho}{\alpha} + \xi^* \right) = 1 - \tau. \quad (\text{SI.5.31})$$

Introduce a change of variables

$$\mu^* := \frac{(1-\tau)(1+\rho)}{\alpha\tau\xi^*}.$$

By combining (SI.5.31) and the characterization in (B.4), we can directly solve for μ and get $\mu^* = q^* \mathcal{M}_{\kappa/\tau}(q^*)$ as given in (SI.5.29). The characterization in (SI.5.30) (for the case of $\tau < 1$) then directly follows from (SI.5.24), (SI.5.28), and (4) after some lengthy calculations.

Next, we consider the case of $\tau > 1$. It is straightforward to verify from (SI.5.6) that

$$\xi = \frac{\tau}{\tau-1} \lambda + \mathcal{O}(\lambda^2).$$

Thus, when $\tau > 1$, $\xi \rightarrow 0$ as $\lambda \rightarrow 0^+$. It follows that

$$\lim_{\lambda \rightarrow 0^+} \nu = \lim_{\lambda \rightarrow 0^+} \left(\frac{1+\rho}{\alpha} + \xi \right) = q^* \quad \text{and} \quad \lim_{\lambda \rightarrow 0^+} \mathcal{M}_\kappa(\nu) = m^*.$$

Substituting these estimates into (SI.5.24), (SI.5.28), and (4), we then reach the characterizations in (SI.5.30) for the case of $\tau > 1$.

SI.5.3 The Generalization Error of In-Distribution Generalization

In what follows, we derive the asymptotic limit of the generalization error for the IDG task.

Result 7. *Consider the test distribution $\mathcal{P}_{\text{test}}$ associated with the IDG task. We have*

$$e(\Gamma^*) \simeq e^{\text{IDG}}(\tau, \alpha, \kappa, \rho, \lambda) := \tau \frac{\rho + \nu - \nu^2 \mathcal{M}_\kappa(\nu) - \xi [1 - 2\nu \mathcal{M}_\kappa(\nu) - \nu^2 \mathcal{M}'_\kappa(\nu)]}{\tau - [1 - 2\xi \mathcal{M}_\kappa(\nu) - \xi^2 \mathcal{M}'_\kappa(\nu)]}, \quad (\text{SI.5.32})$$

where ξ the unique positive solution to the self-consistent equation (SI.5.6) and ν is the constant given in (SI.5.8).

Similar to our derivation of Result 5, we only need to use (SI.5.3) and (SI.5.4) to characterize the asymptotic limits of the first and second terms on the right-hand side of (SI.5.23). Note that, for the IDG task, $A_{\text{test}} = A_{\text{tr}}$. It follows from (SI.5.3) and (SI.5.20) that

$$\frac{1}{d} \text{tr}(\Gamma^* A_{\text{test}}^\top) \simeq 1 - \nu + \nu^2 \mathcal{M}_\kappa(\nu). \quad (\text{SI.5.33})$$

Similarly, since $B_{\text{test}} = E_{\text{tr}}$, we can verify from (SI.5.5) that

$$\begin{aligned} \frac{1}{d} \text{tr} \left(\Gamma_{\text{eq}}^* B_{\text{test}} (\Gamma_{\text{eq}}^*)^\top \right) &= \frac{1}{d} \text{tr}(\Gamma_{\text{eq}}^* A_{\text{tr}}^\top) - \frac{\xi}{d} \text{tr}(\Gamma_{\text{eq}}^* (\Gamma_{\text{eq}}^*)^\top) \\ &\simeq 1 - \nu + \nu^2 \mathcal{M}_\kappa(\nu) - \xi [1 - 2\nu \mathcal{M}_\kappa(\nu) - \nu^2 \mathcal{M}'_\kappa(\nu)], \end{aligned} \quad (\text{SI.5.34})$$

where the second step follows from (SI.5.20) and (SI.5.21). Moreover,

$$\frac{1}{d} \text{tr} \left(B_{\text{test}} \left[(E_{\text{tr}} + \xi I)^{-1} - \xi (E_{\text{tr}} + \xi I)^{-2} \right] \right) = 1 - 2\xi \mathcal{M}_\kappa(\nu) - \xi^2 \mathcal{M}'_\kappa(\nu). \quad (\text{SI.5.35})$$

Substituting (SI.5.34) and (SI.5.35) into (SI.5.4), we have

$$\begin{aligned} &\frac{1}{d} \text{tr}(\Gamma^* B (\Gamma^*)^\top) \\ &\simeq \tau \frac{\rho + \nu - \nu^2 \mathcal{M}_\kappa(\nu) - \xi [1 - 2\nu \mathcal{M}_\kappa(\nu) - \nu^2 \mathcal{M}'_\kappa(\nu)]}{\tau - [1 - 2\xi \mathcal{M}_\kappa(\nu) - \xi^2 \mathcal{M}'_\kappa(\nu)]} + 2(1 - \nu + \nu^2 \mathcal{M}_\kappa(\nu)) - (1 + \rho). \end{aligned}$$

The final result in (SI.5.32) then follows from combining the above expression with (SI.5.33) and (SI.5.23).

Finally, we derive the ridgeless limit of the characterization given in Result 7.

Result 8. *Let q^* , m^* , and μ^* be the scalars defined in (SI.5.29). We have*

$$\begin{aligned} e_{\text{ridgeless}}^{\text{IDG}} &:= \lim_{\lambda \rightarrow 0^+} e^{\text{IDG}}(\tau, \alpha, \kappa, \rho, \lambda) \\ &= \begin{cases} \frac{\tau}{1-\tau} \left(\frac{\rho + q^* - 2q^*(1-\tau)(q^*/\xi^* + 1)}{1-p^*(1-\tau)} + \frac{\tau \mu^* (q^* + \xi^*)^2}{q^*} \right) & \tau < 1 \\ \frac{\tau}{\tau-1} [\rho + q^*(1 - q^* m^*)] & \tau > 1 \end{cases}, \end{aligned} \quad (\text{SI.5.36})$$

where $\xi^* = \frac{(1-\tau)q^*}{\tau \mu^*}$ and $p^* = (1 - \kappa(\frac{\kappa \xi^*}{1-\tau} + 1)^{-2})^{-1}$.

The derivation of this result closely follows that of Result 6. We analyze the cases of $\tau < 1$ and $\tau > 1$ separately. For $\tau < 1$, the equation in (SI.5.6) simplifies to (SI.5.31) as $\lambda \rightarrow 0^+$. For $\tau > 1$, ξ approaches zero as $\lambda \rightarrow 0^+$. Substituting these estimates into (SI.5.32) then yields (SI.5.36) after some detailed calculations.

A Equivalent Statistical Representations

In this appendix, we present an equivalent (but simplified) statistical model for the regression vector H_Z defined in (7). This statistically-equivalent model will simplify the moment calculations in Section SI.2 and the random matrix analysis in Section SI.4.

Lemma 3. *Let w be a given task vector with $\|w\| = \sqrt{d}$. Meanwhile, let $a \sim \mathcal{N}(0, 1)$, $s \sim \mathcal{N}(0, 1)$, $\epsilon \sim \mathcal{N}(0, \rho)$ be three scalar normal random variables, and $q \sim \mathcal{N}(0, I_{\ell-1})$, $g \sim \mathcal{N}(0, I_{d-1})$, $u \sim \mathcal{N}(0, I_{d-1})$, and $v_\epsilon \sim \mathcal{N}(0, \rho I_\ell)$ be isotropic normal random vectors. Moreover, w and all of the above random variables are mutually independent. We have the following equivalent statistical representation of the pair $(H_Z, y_{\ell+1})$:*

$$H_Z \stackrel{(d)}{=} (d/\ell)M_w \begin{bmatrix} s \\ u \end{bmatrix} \left[h^\top M_w, \quad (a/\sqrt{d} + \theta_\epsilon)^2/\sqrt{d} + \theta_q^2/\sqrt{d} \right], \quad (\text{A.1})$$

and

$$y_{\ell+1} \stackrel{(d)}{=} s + \epsilon. \quad (\text{A.2})$$

In the above displays, M_w denotes a symmetric and orthonormal matrix such that

$$(M_w)e_1 = \frac{w}{\|w\|}, \quad (\text{A.3})$$

where e_1 denotes the first natural basis vector in \mathbb{R}^d ; $h \in \mathbb{R}^d$ is a vector defined as

$$h := \begin{bmatrix} \frac{\theta_\epsilon a}{\sqrt{d}} + \frac{a^2}{d} + \theta_q^2 \\ [(\theta_\epsilon + a/\sqrt{d})^2 + \theta_q^2]^{1/2} g/\sqrt{d} \end{bmatrix}; \quad (\text{A.4})$$

and $\theta_\epsilon, \theta_q$ are scalars such that

$$\theta_\epsilon = \|v_\epsilon\|/\sqrt{d} \quad \text{and} \quad \theta_q = \|q\|/\sqrt{d}.$$

Remark 7. *For two random variables A and B , the notation $A \stackrel{(d)}{=} B$ indicates that A and B have identical probability distributions. Note that A and B can be either scalars [as in the case of (A.2)], or matrices of matching dimensions [as in the case of (A.1)].*

Remark 8. *A concrete construction of the symmetric and orthonormal matrix M_w satisfying (A.3) can be based on the Householder transformation [54–56].*

Proof. Recall that the data vector $x_{\ell+1}$ is independent of the task vector w . Then, by the rotational symmetry of the isotropic normal distribution, we can rewrite

$$x_{\ell+1} \stackrel{(d)}{=} \frac{1}{\sqrt{d}}M_w \begin{bmatrix} s \\ u \end{bmatrix}, \quad (\text{A.5})$$

where $s \sim \mathcal{N}(0, 1)$ and $u \sim \mathcal{N}(0, I_{d-1})$ are two independent normal random variables (vectors), and M_w is the symmetric orthonormal matrix specified in (A.3). Note that $y_{\ell+1} = x_{\ell+1}^\top w + \epsilon$, with $\epsilon \sim \mathcal{N}(0, \rho)$ denoting the noise. The representation in (A.2) then follows immediately from (A.5) and the identity in (A.3).

To show (A.1), we first reparameterize the $d \times \ell$ Gaussian data matrix X as

$$X = M_w \begin{bmatrix} a & q^\top \\ p & U \end{bmatrix} M_{v_\epsilon} / \sqrt{d}. \quad (\text{A.6})$$

In the above display, $a \sim \mathcal{N}(0, 1)$, $p \sim \mathcal{N}(0, I_{d-1})$, $q \sim \mathcal{N}(0, I_{\ell-1})$; $U \in \mathbb{R}^{(d-1) \times (\ell-1)}$ is a matrix with iid standard normal entries; and M_{v_ϵ} is a symmetric orthonormal matrix such that

$$M_{v_\epsilon} e_1 = \frac{v_\epsilon}{\|v_\epsilon\|}, \quad (\text{A.7})$$

where e_1 denotes the first natural basis vector in \mathbb{R}^ℓ . Since the data matrix X , the task vector w , and the noise vector v_ϵ are mutually independent, it is straightforward to verify via the rotational symmetry of the isotropic normal distribution that both sides of (A.6) have identical probability distributions. Using this new representation, we have

$$X v_\epsilon = \theta_\epsilon M_w \begin{bmatrix} a \\ p \end{bmatrix}.$$

Meanwhile,

$$X^\top w = M_{v_\epsilon} \begin{bmatrix} a \\ q \end{bmatrix}, \quad (\text{A.8})$$

and thus

$$X X^\top w = \frac{1}{\sqrt{d}} M_w \begin{bmatrix} a^2 + \|q\|^2 \\ ap + Uq \end{bmatrix}. \quad (\text{A.9})$$

Combining (A.8) and (A.9) yields

$$\begin{aligned} Xy &= X X^\top w + X v_\epsilon \\ &= M_w \begin{bmatrix} \theta_\epsilon a + a^2/\sqrt{d} + \theta_q^2 \sqrt{d} \\ (\theta_\epsilon + a/\sqrt{d})p + Uq/\sqrt{d} \end{bmatrix}. \end{aligned}$$

Observe that $Uq/\sqrt{d} \stackrel{(d)}{=} \theta_q p'$, where $p' \sim \mathcal{N}(0, I_{d-1})$ is a normal random variable independent of everything else. Using this reparametrization for Uq/\sqrt{d} and the fact that p, p' are two independent Gaussian vectors, we can conclude that

$$\frac{1}{\sqrt{d}} Xy \stackrel{(d)}{=} M_w h, \quad (\text{A.10})$$

where h is the random vector defined in (A.4).

Lastly, we consider the term $y^\top y$ in (7). Since $y = X^\top w + v_\epsilon$,

$$\begin{aligned} y^\top y &= \left\| X^\top w + v_\epsilon \right\|^2 \\ &= \left\| X^\top w + \theta_\epsilon \sqrt{d} M_{v_\epsilon} e_1 \right\|^2 \\ &= (a + \theta_\epsilon \sqrt{d})^2 + \theta_q^2 d, \end{aligned} \quad (\text{A.11})$$

where the second equality follows from (A.7) and to reach the last equality we have used the representation in (A.8). To show (A.1), we recall the definition of H_Z in (7). Substituting (A.5), (A.10) and (A.11) into (7), we are done. \square

B The Stieltjes Transforms of Wishart Ensembles

In this appendix, we first recall several standard results related to the Stieltjes transforms of Wishart ensembles. In our problem, we assume that there are k unique task vectors $\{w_i\}_{i \in [k]}$ in the training set. Moreover, these task vectors $\{w_i\}_{i \in [k]}$ are independently sampled from the uniform distribution on the sphere $\mathcal{S}^{d-1}(\sqrt{d})$ with radius \sqrt{d} . Let

$$F_R(\nu) := (R_{\text{tr}} + \nu I_d)^{-1}, \quad (\text{B.1})$$

where R_{tr} is the sample covariance matrix of the task vectors as defined in (SI.4.1) and ν is a positive scalar.

Note that the distribution of R_{tr} is asymptotically equivalent to that of a Wishart ensemble. By standard random matrix results on the Stieltjes transforms of Wishart ensembles (see, *e.g.*, [35]), we have

$$\frac{1}{d} \text{tr} F_R(\nu) \simeq \mathcal{M}_\kappa(\nu) \quad (\text{B.2})$$

as $d, k \rightarrow \infty$ with $k/d = \kappa$. Here,

$$\mathcal{M}_\kappa(\nu) := \frac{2}{\nu + 1 - 1/\kappa + [(\nu + 1 - 1/\kappa)^2 + 4\nu/\kappa]^{1/2}}. \quad (\text{B.3})$$

is the solution to the self-consistent equation

$$\frac{1}{\mathcal{M}_\kappa(\nu)} = \frac{1}{1 + \mathcal{M}_\kappa(\nu)/\kappa} + \nu. \quad (\text{B.4})$$

Moreover,

$$\frac{1}{d} \text{tr} F^2(\nu) \simeq -\mathcal{M}'_\kappa(\nu) = \frac{\mathcal{M}_\kappa^2(\nu)}{1 - \frac{\kappa \mathcal{M}_\kappa^2(\nu)}{[\kappa + \mathcal{M}_\kappa(\nu)]^2}}.$$

For the remainder of this appendix, we will further explore the self-consistent equation given by (SI.4.7). We will show that the solution χ_π and its derivative $\frac{d}{d\pi} \chi_\pi$, at $\pi = 0$, can be characterized by the function $\mathcal{M}_\kappa(\nu)$ in (B.3). To start, note that at $\pi = 0$, the equation in (SI.4.7) can be written as

$$\frac{\tau \chi_0}{1 + \chi_0} = (1 + 1/d) - \frac{\lambda(1 + \chi_0)}{d} \text{tr}(E_{\text{tr}} + \lambda(1 + \chi_0)I)^{-1}. \quad (\text{B.5})$$

Recall the definition of E_{tr} given in (SI.4.3). It is straightforward to verify that

$$(E_{\text{tr}} + \lambda(1 + \chi_0)I_{d+1})^{-1} = \begin{bmatrix} F_R(\nu_0) + a^*(1 + \rho)^2 F_R(\nu_0) b_{\text{tr}} b_{\text{tr}}^\top F_R(\nu_0) & -a^*(1 + \rho) F_R(\nu_0) b_{\text{tr}} \\ -a^*(1 + \rho) b_{\text{tr}}^\top F_R(\nu_0) & a^* \end{bmatrix}, \quad (\text{B.6})$$

where $F_R(\cdot)$ is the function defined in (B.1),

$$\nu_0 = \frac{1 + \rho}{\alpha} + \lambda(1 + \chi_0) \quad (\text{B.7})$$

and

$$\frac{1}{a^*} = (1 + \rho)^2 + \lambda(1 + \chi_0) - (1 + \rho)^2 b_{\text{tr}}^\top F_R(\nu_0) b_{\text{tr}}. \quad (\text{B.8})$$

From (B.6), the equation (B.5) becomes

$$\frac{\tau \chi_0}{1 + \chi_0} = (1 + 1/d) - \frac{\lambda(1 + \chi_0)}{d} \text{tr} F_R(\nu_0) - (1 + \rho)^2 \frac{a^* \lambda(1 + \chi_0)}{d} \|F_R(\nu_0) b_{\text{tr}}\|^2. \quad (\text{B.9})$$

By the construction of $F_R(\nu_0)$ and b_{tr} , we can verify that

$$b_{\text{tr}}^\top F_R(\nu_0) b_{\text{tr}} \leq 1 \quad \text{and} \quad \|F_R(\nu_0) b_{\text{tr}}\|^2 \leq \frac{1}{\nu_0} \leq \frac{\alpha}{1+\rho}. \quad (\text{B.10})$$

Substituting the first inequality above into (B.8) gives us

$$a^* \lambda(1 + \chi_0) \leq 1.$$

Combining this estimate with the second inequality in (B.10), we can conclude that the last term on the right-hand side of (B.9) is negligible as $d \rightarrow \infty$. Moreover, using the asymptotic characterization given in (B.2), the equation (B.9) leads to

$$\frac{\tau \chi_0}{1 + \chi_0} \simeq 1 - \lambda(1 + \chi_0) \mathcal{M}_\kappa(\nu_0). \quad (\text{B.11})$$

Introducing a change of variables

$$\xi_0 = \lambda(1 + \chi_0),$$

and also recalling the definition of ν_0 in (B.7), we can further transform (B.11) to

$$\xi_0 \mathcal{M}_\kappa \left(\frac{1 + \rho}{\alpha} + \xi_0 \right) - \frac{\tau \lambda}{\xi_0} \simeq 1 - \tau.$$

Observe that the above is identical to the equation in (SI.5.6), except for a small error term captured by \simeq . By the stability of (SI.5.6), we can then conclude that

$$\xi_0 \simeq \xi, \quad (\text{B.12})$$

thus verifying (SI.5.15).

Next, we compute χ'_0 , the derivative of χ_π (with respect to π) evaluated at $\pi = 0$. Differentiating (SI.4.7) give us

$$\tau \chi'_0 = \frac{1}{d} \text{tr} \left[(E_{\text{tr}} + \xi_0 I)^{-1} \left(\chi'_0 E_{\text{tr}} - \frac{(1 + \chi_0)^2}{\tau} B_{\text{test}} \right) (E_{\text{tr}} + \xi_0 I)^{-1} E_{\text{tr}} \right]. \quad (\text{B.13})$$

Thus,

$$\frac{\tau \chi'_0}{(1 + \chi_0)^2} \simeq \frac{\frac{1}{d} \text{tr} (B_{\text{test}} [(E_{\text{tr}} + \xi I)^{-1} - \xi (E_{\text{tr}} + \xi I)^{-2}])}{1 - 2\xi \text{tr} (E_{\text{tr}} + \xi I)^{-1} / d + \xi^2 \text{tr} (E_{\text{tr}} + \xi I)^{-2} / d - \tau}, \quad (\text{B.14})$$

where we have used (B.12) to replace ξ_0 in (B.13) by ξ , with the latter being the solution to the self-consistent equation in (SI.5.6). Using the decomposition in (B.6) and following similar arguments that allowed us to simplify (B.9) to (B.11), we can check that

$$\frac{1}{d} \text{tr} (E_{\text{tr}} + \xi I)^{-1} \simeq \frac{1}{d} \text{tr} S (E_{\text{tr}} + \xi I)^{-1} S^\top \simeq \frac{1}{d} \text{tr} F \left(\frac{1 + \rho}{\alpha} + \xi \right) \simeq \mathcal{M}_\kappa \left(\frac{1 + \rho}{\alpha} + \xi \right), \quad (\text{B.15})$$

and

$$\frac{1}{d} \text{tr} (E_{\text{tr}} + \xi I)^{-2} \simeq \frac{1}{d} \text{tr} S (E_{\text{tr}} + \xi I)^{-2} S^\top \simeq \frac{1}{d} \text{tr} F^2 \left(\frac{1 + \rho}{\alpha} + \xi \right) \simeq -\mathcal{M}'_\kappa \left(\frac{1 + \rho}{\alpha} + \xi \right), \quad (\text{B.16})$$

where S is a $d \times (d+1)$ matrix obtained by removing the last row of I_{d+1} , and $\mathcal{M}_\kappa(\cdot)$ is the function defined in (B.3). Substituting (B.15) and (B.16) into (B.14) yields

$$\frac{\tau \chi'_0}{(1 + \chi_0)^2} \simeq \frac{\frac{1}{d} \text{tr} (B_{\text{test}} [(E_{\text{tr}} + \xi I)^{-1} - \xi (E_{\text{tr}} + \xi I)^{-2}])}{1 - 2\xi \mathcal{M}_\kappa \left(\frac{1 + \rho}{\alpha} + \xi \right) - \xi^2 \mathcal{M}'_\kappa \left(\frac{1 + \rho}{\alpha} + \xi \right) - \tau}. \quad (\text{B.17})$$